1960

Some dynamic creep characteristics of gypsum

Ikram-Ul-Haq Dar

SOME DYNAMIC CREEP CHARACTERISTICS OF GYPSUM

BY

IKRAM-UL-HAQ DAR

A

THESIS

submitted to the faculty of the

SCHOOL OF MINES AND METALLURGY OF THE UNIVERSITY OF MISSOURI

in partial fulfillment of the work required for the

Degree of

MASTER OF SCIENCE IN MINING ENGINEERING

Rolla, Missouri

1960

Approved by

Rodney D. Cander (Advisor) Paul Dean Proctor

James C. Maxwell Carl R. Christiansen

ABSTRACT

A review of literature concerned with time-dependent deformation of geologic and non-geologic materials is presented. A static loading machine and a four unit dynamic loading unit was designed and assembled to evaluate static and dynamic creep properties of gypsum. The tests were run for various levels of static loads, and superimposed dynamic loads. Investigations were carried out to determine the relationships, if any, between impact energy, impact velocity and momentum, and dynamic strains. Viscoelastic coefficients were determined for the investigations. The conclusion was presented that time-dependent strain in the dynamic creep tests of the particular gypsum rock tested is a function of impact momentum within the elastic limit of the material.

ACKNOWLEDGEMENT

The author takes this opportunity to express his sincere appreciation to Dr. G. B. Clark, Chairman of the Department of Mining Engineering, University of Missouri, School of Mines and Metallurgy, for suggesting the problem and his valuable advice and to Professor R. D. Caudle of the Department of Mining Engineering, for help and advice throughout the investigation, and for his criticism of the manuscript.

The author wishes to offer sincere thanks to Professor R. F. Bruzewski, of the Department of Mining Engineering, for his advice and assistance in the preparation of the pictures contained in this paper.

TABLE OF CONTENTS

Page

LIST OF ILLUSTRATIONS

Figure Page

CHAPTER I

THE PROBLEM AND DEFINITION OF TERMS USED

The choice of method of extraction of geologic materials from the earth's crust is dependent largely upon their physical properties. One important physical characteristic of rock, its time-dependent deformation under load, has generally been neglected in the past in the engineering studies conducted to determine an optimum mining method. The reasons for this neglect have been the generally low level of pressures encountered in previous mine workings, the high resistance to deformation of the rock commonly encountered, and the lack of definite information on the creep properties of rock.

The extension of mine workings, in general, to greater depths, and recent proposals for mining of relatively weak sedimentary materials, such as gypsum, at previously untried depths, in particular, has developed a special need for information concerning the creep characteristics of rock. A few investigations have been made with regard to the time-dependent behavior of rocks under static loading conditions. However, there has been no work done to date to determine the effects of repeated impact loads superimposed on the static loads.

The Problem

Statement of the Problem

It was the purpose of this study to determine the dynamic characteristics of gypsum when subjected to repeated impact loads superimposed upon a steady-state loading. The determination of any conclusions which might be applied to the dynamic time-dependent behavior of rocks in general, from the data obtained, was of primary interest.

Specific relationships which were to be considered were the effect of (1) static load level, (2) drop mass, (3) height of drop mass, and (4) quantities such as drop mass velocity, energy, and momentum, upon the creep characteristics of gypsum.

Importance of the Study

The extension of mining practice to deeper levels have magnified the problems of rock bursts, ground failure and rock creep, considerably. Creep of materials has largely been a study of deformation under long-time static loads. Pressures corresponding to these static loads are developed in the rock surrounding mine openings underground as a result of the weight of overlying materials and the tectonic forces associated with geologic displacements. In addition to these static loadings, the mine rock is periodically subjected to dynamic loads. Large scale transient loads are experienced due to blasting and pneumatic drilling operations, producing repeated impact loads. Recent military interest in permanent underground installations has been concerned with the effect of possible dynamic loadings on the structure as well as the pre-existing static stresses. The effect of these dynamic loadings upon the pre-stressed rock has not been previously evaluated.

An understanding of the time-dependent behavior of rock under repeated dynamic loads is essential to successful mining in the future.

It will also be very useful in the further development of research in the fields of ground failure, comminution, explosives and seismology.

Procedure of the Study

The investigation was performed in four stages (1) a review of literature concerned with the creep of both geologic and non-geologic materials under static and dynamic loadings; (2) the design of static and dynamic loading devices, and strain measuring instrumentation for creep tests of rock cylinders; (3) static and dynamic creep tests of gypsum rock; and (4) evaluation of the data obtained and comparison with available pertinent data in the literature.

Definitions of Terms Used

Creep. Both geologic and non-geologic materials may exhibit time-dependent-deformation under the application of long-term static or dynamic loads. This deformation is termed creep.

Ductility. The quantitative measure of the ability of a plastic body to undergo large deformations without fracture. (15)*

Plasticity. The property which permits materials to undergo permanent change in shape without fracture or notable loss of cohesion.

Rheology. The study of deformation and flow in materials.

Stress. The internal force per unit of area which resists a change in size or shape of a body.

Strain. If the magnitude of deformation is small compared to the dimensions of a body, strain in a particular direction may be defined as the deformation in that direction divided by the length over which that deformation was measured.

Dynamic modulus of elasticity. The effective stress-to-strain ratio during a vibration.

Elasticity. The ability of a substance to deform under an applied load, and resume its original shape immediately and completely upon removal of load.

Viscosity. The ability of a substance to deform at a constant rate under a static load.

*Refers to the bibliographical entry.

CHAPTER II

REVIEW OF LITERATURE

The review of published creep test data has been divided into two major sections (1) time-dependent deformation under static loadings and (2) time-dependent deformation under dynamic loadings. Creep studies have been performed on both geologic and non-geologic materials. A detailed review of investigations of time-dependent deformation of rocks under static loads has been presented together with a summary of pertinent literature in the field of non-geologic materials. There is little published material available concerned with creep of geologic materials under dynamic loadings. For this reason an extensive review of the behavior of metals under extended periods of dynamic loading has been included.

The study of the time-dependent deformation of materials has been conducted on several different planes; that is, empirically, phenomenologically, and theoretically.

Time-Dependent Deformation under Static Loadings

The deformation of a solid under a long-period stress is known as time-dependent deformation. Time-dependent deformation which occurs at a level of stress below the elastic limit of a solid is defined as creep.

Creep of Geologic Materials

Most geologic materials exhibit a slow plastic deformation under long term applied stress, known as time-strain or creep. Hardy (13) stated that the behavior of such materials can be successfully explained by the theories postulated for non-geologic materials.

Empirical treatment. An empirical approach deals with conclusions based on the experimental evidence. The experimental results are fitted to known empirical equations or to new equations developed to suit the particular case. When applied to the study of creep, this approach does not give any information as to the actual mechanism of the deformation process. However, its use permits the establishment of equations which may be used to predict the behavior of a material under load.

Uniaxial creep tests. The pioneer work in the field of rock creep was that of D. T. Griggs (9). He recognized that materials may support without permanent set, shear stresses of short duration, and yet yield continually when subjected to smaller stresses for long periods of time. It was noted that some rocks, notably clays and shales, flow slowly or "creep" under relatively light loads acting over a number of years, but that other rocks do not creep appreciably under much higher stresses applied over the same period of time. These latter rocks however, exhibited the properties of plastic flow when high differential stresses were applied, together with high confining pressures.

Griggs considered flow to have occurred whenever a body was so strained that the deformation did not instantly disappear on the removal of the external forces; if this deformation did not result in a notable loss of cohesion.

It was stated that a solid may creep or deform continuously when subjected to constant differential stress. Griggs termed this deformation 'Elastico Viscous Flow' and described it as an aggregate effect of two types of flow.

(1) Pseudoviscous flow.---deformation at a constant rate, given by Ct; and

(2) Elastic flow.---deformation decreasing logarithmically with time given by B log t.

The total strain $\left(\frac{-\Delta L}{L_0}\right)$ after time t was given by an equation of the form (9, p. 225):

$$S = A + B \log t + Ct \qquad (1)$$

where t is time, and A, B and C were constants depending on type of material used.

Upon removal of the load from the specimen a recovery curve was obtained, which was found to have an equation of the form (9, p. 225):

$$S' = A' + B \log t \qquad (2)$$

This behavior is apparent from Figure 1. Differentiating equation (1) with respect to time gave the following:

$$\dot{S} = B/t + C \text{ where } \dot{S} = dS/dt. \qquad (3)$$

From equation (3) it was shown that the rate of elastic flow decreased inversely with time until it became small relative to the pseudoviscous flow. The deformation then continued with a rate of $\dot{S} \approx C$.

The pseudoviscous flow proposed by Griggs resembled viscous flow in liquids to the extent that the rate of shear was constant under constant stress. By the use of standard equations of elasticity and Jeffreys (16) term for elastic-viscous flow, an expression can be developed for the equivalent viscosity of rock namely (16, p. 265):

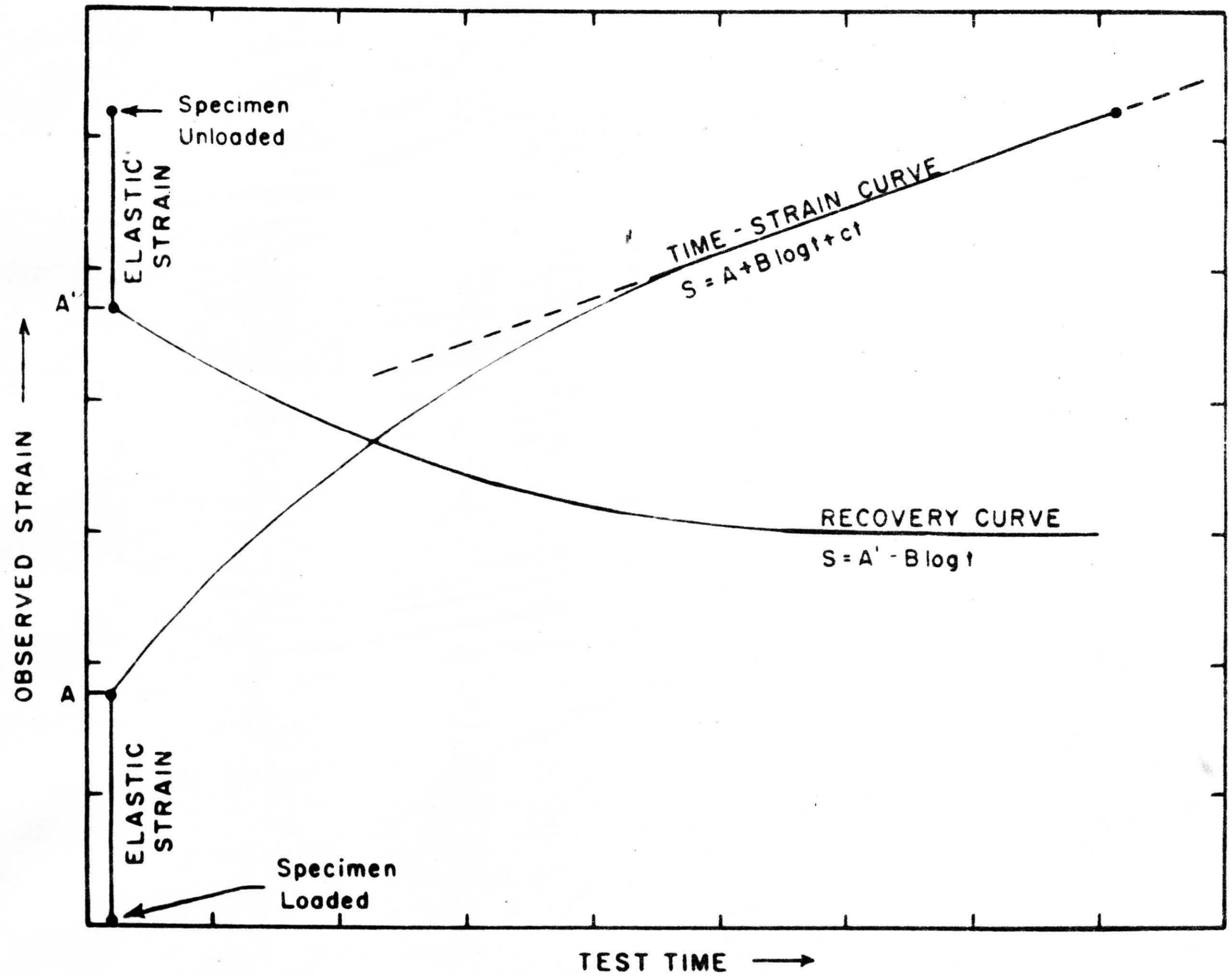

FIGURE 1. Typical time-strain and recovery curves for elastico-viscous material.
(After Hardy, 1959)

$$\overset{*}{n} = P/3\,(dS/dt) \qquad (4)$$

where $\overset{*}{n}$ is the equivalent viscosity, P is the applied compressive stress and $(dS/dt)_{II}$ is the strain rate in the pseudoviscous region.

Griggs (9) tested a specimen of Solonhofen limestone in a sensitive creep tester for a period of a year and a half under a pressure of 1400 kg/cm^2. The ultimate static compressive strength of this particular limestone was 2,560 kg/cm^2. The rock showed a continuous flow at a decreasing rate, as shown in Figure 2, forming a straight line on a semi-log paper. The equation of the straight line was found to be:

$$S = (6.10 + 5.20 \log t)\, 10^{-5}$$

where S is the shortening per unit length and t the time in days. Pseudoviscous flow was not observed as a part of the deformation. If present it was so small that the sensitivity of the measurements did not distinguish it.

Among recent attempts to analyze the creep of rocks by use of an empirical approach has been that of Lomnitz (19). In testing two igneous rocks in torsion, he found the following relationship between maximum shear strain γ, maximum shear stress τ and time t days over a ten day test (19, p 473).

$$\text{Granodiorite:} \quad \gamma = \frac{\tau}{29 \times 105} \quad 1 + 0.010'' \,(1 + t/86.4) \qquad (5)$$

$$\text{Gabbro:} \quad \gamma = \frac{\tau}{58 \times 105} \quad 1 + 0.003'' \,(1 + t/86.4) \qquad (6)$$

<u>Triaxial creep tests</u>. Griggs (8) found that the elastic limit of rock subjected to long term load was changed only slightly by

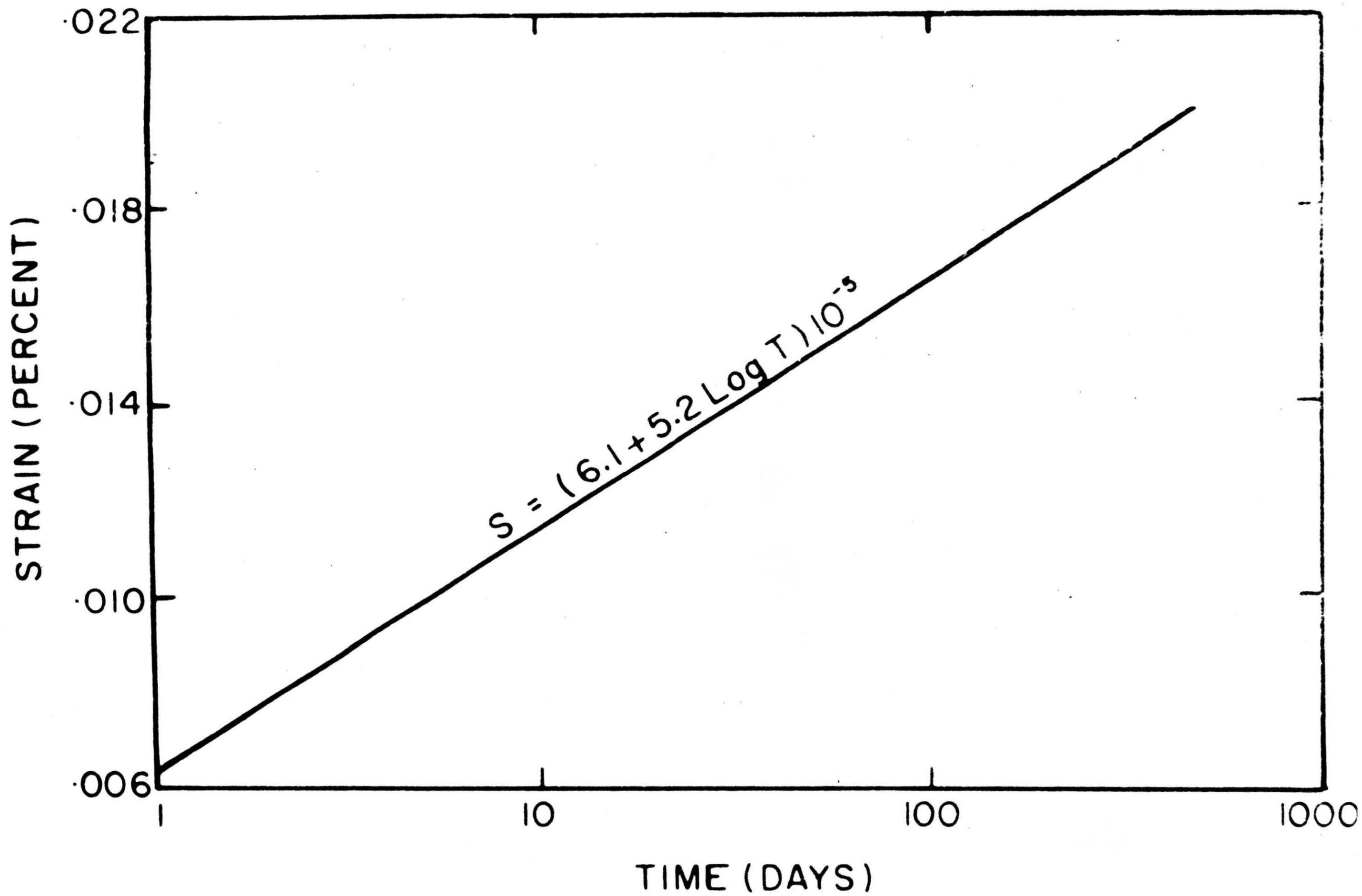

FIGURE 2. Time-strain curve for Solenhofen limestone under uniaxial compressive stress of 1400 Kg/cm². (After Griggs, 1939)

applying a confining pressure to the specimen. A confining pressure of 10,000 atmospheres raised the elastic limit of Solenhofen limestone about 10 percent. The ultimate strength, however was very greatly changed as shown in Figure 3. A pressure of 10,000 atmospheres increased the ultimate strength more than 600 percent.

A limestone specimen, under a confining pressure of 10,000 atmospheres, was subjected to a varying differential load increasing to a certain value, and then held constant while the plastic deformation was observed as a function of time. Then the differential load was increased to a higher value and the process repeated. At low values of the differential force, no plastic deformation took place, regardless of time. For higher values, it was found that the rate of plastic deformation varied in proportion to the applied force. The time strain figures were found to be very similar to those obtained for metals at high temperatures.

It was expected that a rock would be more ductile when deformed slowly than quickly. Just the opposite was found experimentally. Figure 4 shows the amount of plastic deformation before rupture in a series of similar specimens, versus time to failure. Similar conditions of temperature and confining pressures were maintained, with a different rate of increase of differential pressure for each specimen. From this data, Griggs concluded that an increase in duration of the static test decreases plastic yield before rupture, and, therefore, where crystalline rocks occur at great depths and pressures, it is not necessary to have a sudden increase of differential stress to cause

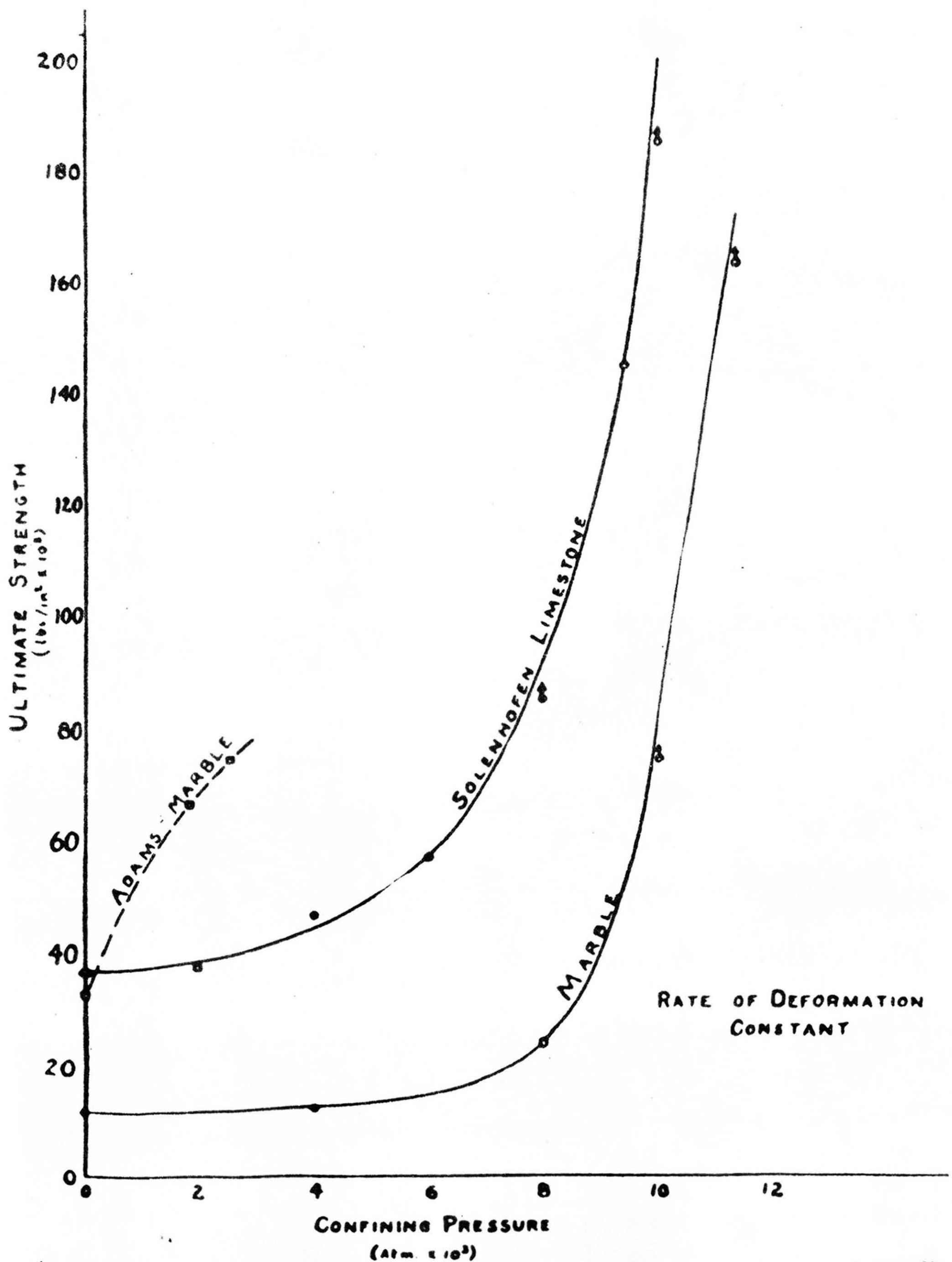

Figure 3. Effect of confining pressure on ultimate strength of rocks. (After Griggs, 1936)

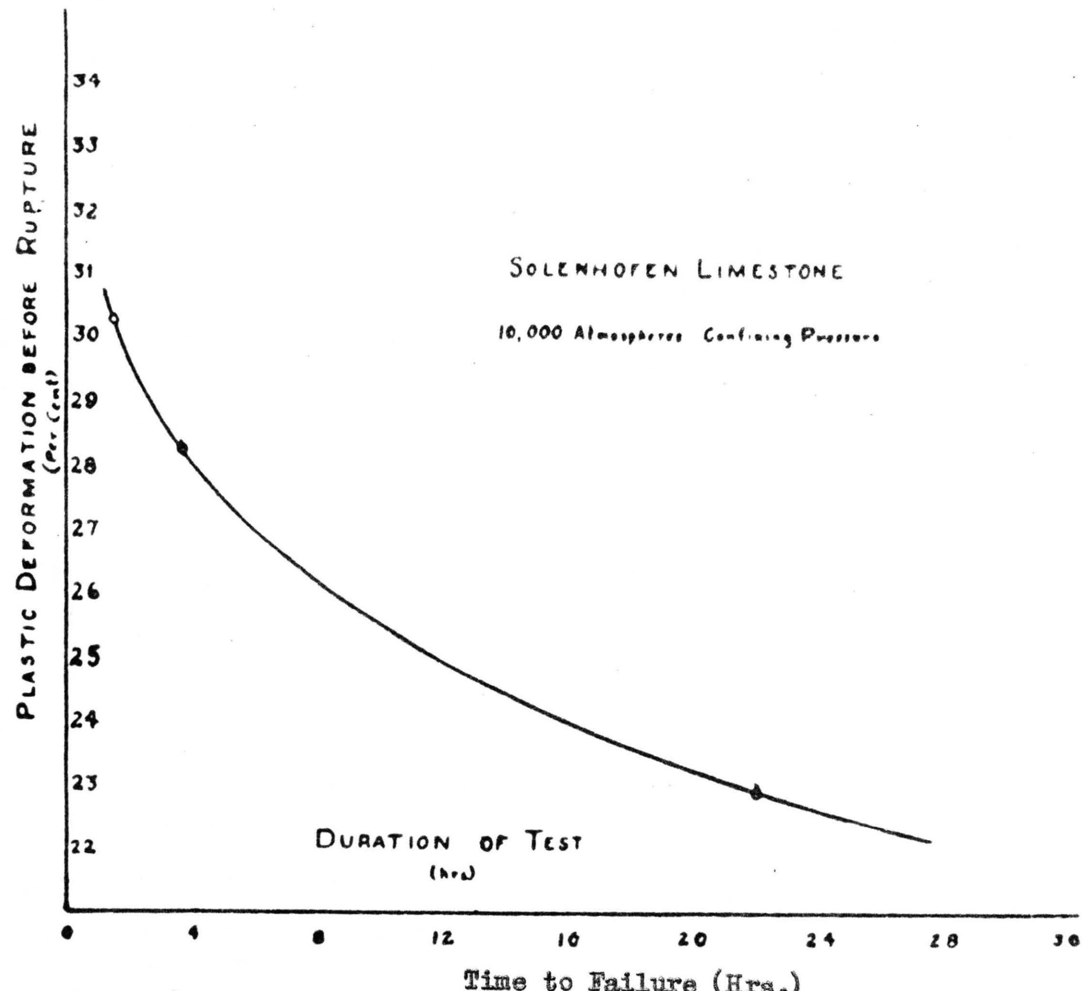

Figure 4. Time strain curve for Solenhofen limestone under 10,000 confining pressure (After Griggs, 1936)

fracture. A long term differential stress above the fundamental strength would be sufficient for failure.

The variation of strength and ductility with confining pressures for a number of sedimentary rocks has been studied recently by Handin and Hager (15). These tests indicate, Figure 5, that both ductility and strength increases with confining pressure, although not always in a directly proportional manner.

Phenomenological treatment. This approach expresses an anology to the behavior of a material in terms of simple physical models, which serve to illustrate the properties of a more or less complicated structure. Hardy (12, 14) using the phenomenological approach, conducted a series of experiments on a weakly cohesive iron ore from Steep Rock Lake, Ontario. His experiments indicated that some types of rocks may be classified as viscoelastic, and for these particular rocks a phenomenological treatment can be successfully applied in order to explain their behavior. Figure 6 shows the complete deformation recovery curve for a Steep Rock iron ore specimen, illustrating the equivalence of the rock specimen and phenomenologic model. A complete discussion of the phenomenological approach to time-dependent deformation of materials is presented under Creep of Non-Geologic Material in this chapter.

Mechanisms of Rock Creep. Several mechanisms of rock creep have been proposed. Griggs (8) tested a marble specimen and obtained under a confining pressure of 10,000 atmospheres and 150°C, a shortening of 30 percent before fracture, with a differential stress of 8100 kg/cm^2. However when a similar specimen was tested under a confining

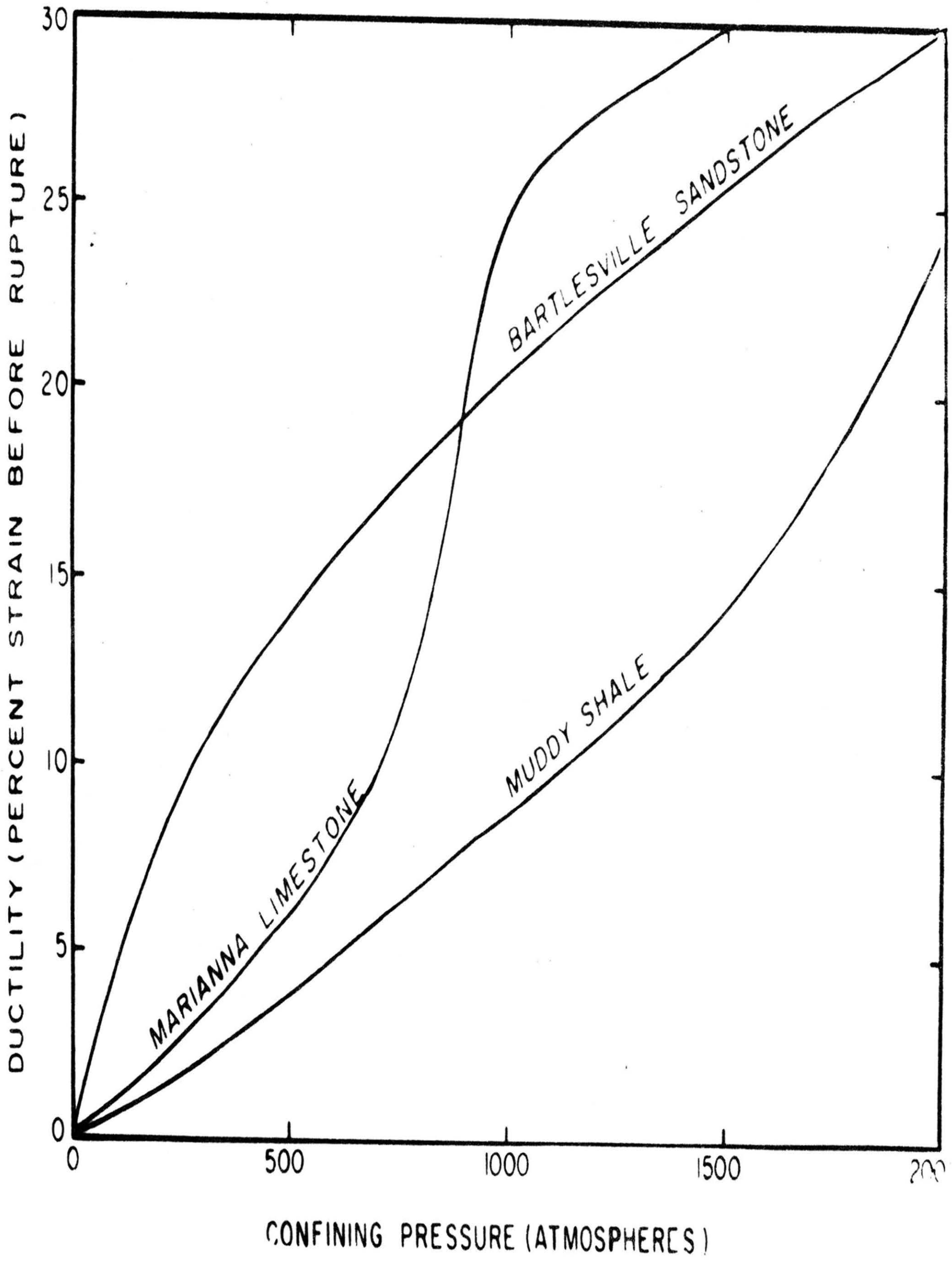

FIGURE 5. Effect of confining pressure on ductility. (After Handin and Hager, 1957.)

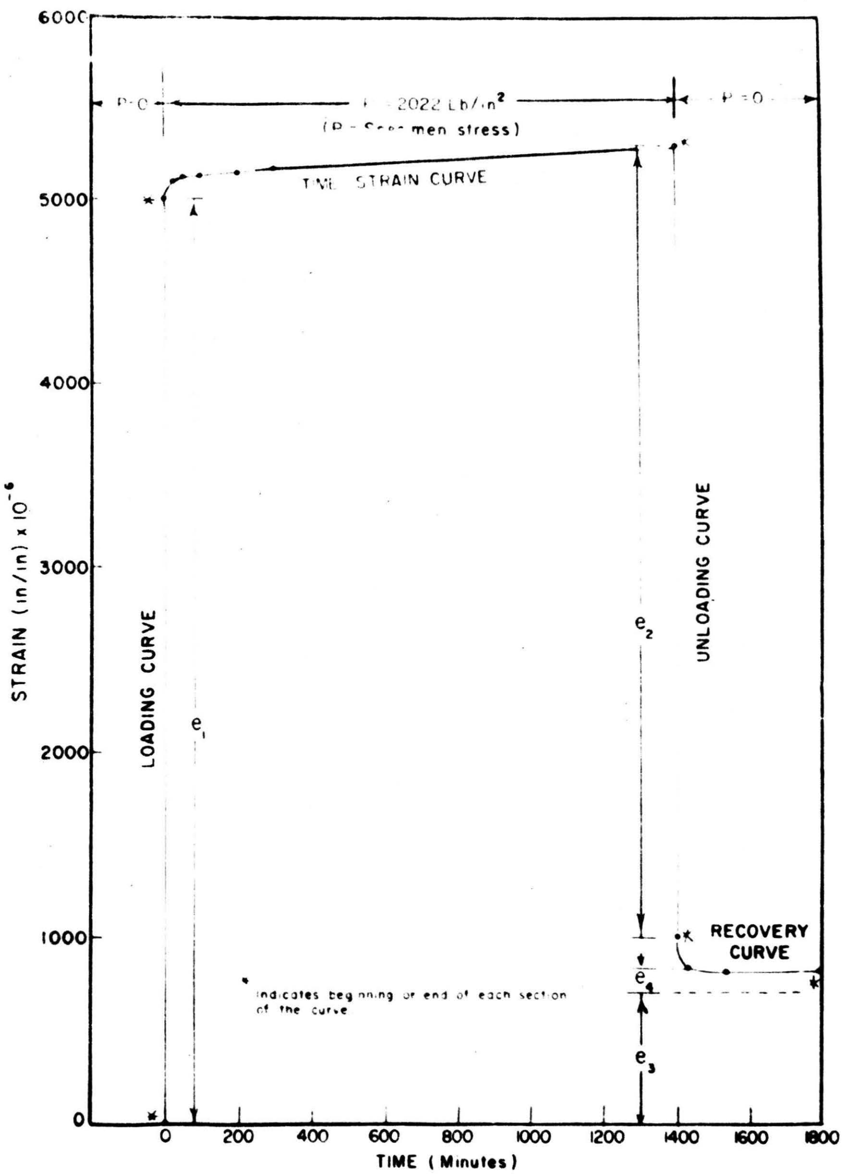

FIGURE 6. Deformation-recovery curve for Steep Rock Lake iron ore, under uniaxial stress of 2022 psi and at room temperature. (After Hardy, 1959.)

pressure of 10,000 atmospheres and 150°C, surrounded with carbonated water, a differential stress of only 1500 kg/cm^2 was required for the same percentage of shortening. The presence of water and CO_2 seemed to favor solution and recrystallization of individual calcite grains. Deformation was assumed to have proceeded by recrystallization flow.

Russell (27) showed experimentally that stresses may be localized within a single crystal, and that because of this, solution and recrystallization may take place within a crystal grain under localized stress with consequent flattening normal to the direction of compression. In these experiments the crystal was in contact with a saturated solution of the same chemical composition. To test the validity of the above statement, Griggs (10) carried out numerous tests on alabaster. All experiments were conducted at room temperature, and in each test a specific constant differential stress was applied to determine the effects of differential pressure on the properties of flow. The specimens were tested while surrounded and in contact with various liquid solutions.

Griggs (11) suggested that the elastic flow portion of rock creep is due to rearrangement of atoms in the region of structural inhomogeneities. These atoms move relatively slowly to new equilibrium positions when external stress is changed. Griggs believed that psuedoviscous flow in some metals may be explained by a process of solid diffusion, but other processes of flow such as intergranular and intercrystalline motion observed in lead may be more pronounced in rock. Flow recrystallization has also been suggested, as was mentioned previously.

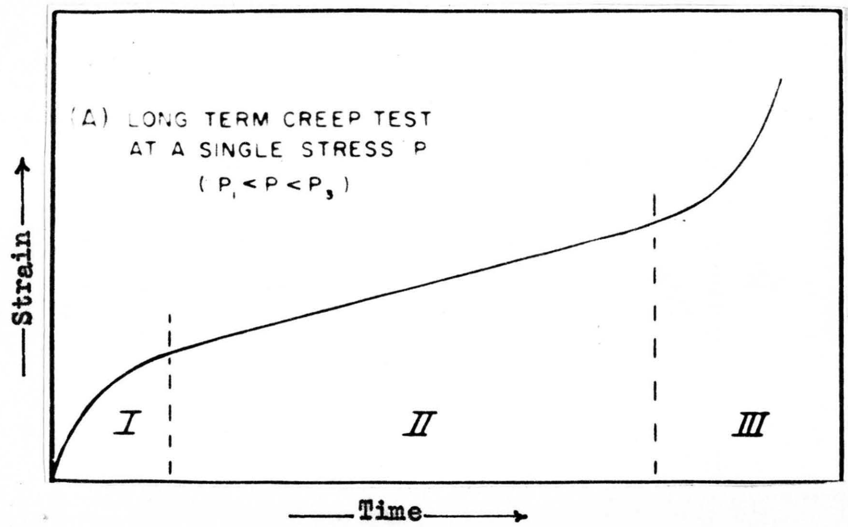

Figure 7. Typical Curve Illustrating Long Term Creep Test at Stress p.

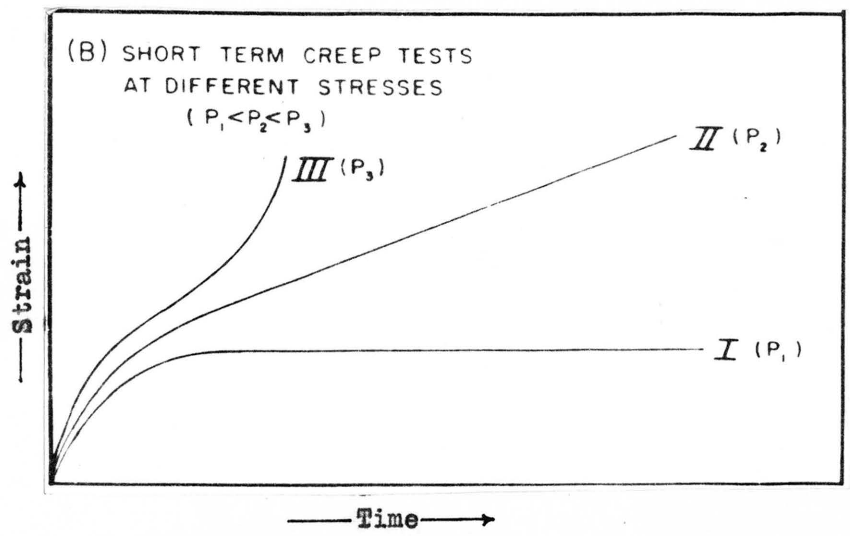

Figure 8. Curve Illustrating Creep Behavior under Different Stresses for Short Periods of Time.

Several investigators have shown that primary creep in metals for most cases can be represented accurately by (12, p. 147):

$$\dot{S} = Bt^{-m} \qquad (7)$$

where S is the strain, t the time, B and n are constants determined from a creep experiment, and where $0 \leqslant m \leqslant 1$. When equation 7 is fitted to the experimental creep curves a few specific values of m fit a majority of the curves. Taking m = 1 leads to the frequently observed logarithmic creep law.

$$S = B \log t \quad (t > 1) \qquad (8)$$

where B is a constant for a particular material. This was observed by Phillips (23) for rubber, glass, and various metals and has since been confirmed by Davis and Thomson (4).

Materials which exhibit faster creep rates and relatively large strains, require a value of m less than unity to fit the strain-time curves. The value 2/3 leads to Andrade's creep law:

$$S = \overset{*}{B}t^{1/3} \text{ where } \overset{*}{B} \text{ is a constant.} \qquad (9)$$

Andrade (1) showed that this relationship was obeyed by some polycrystalline metals within the primary portion of the creep curve. He observed that it was necessary to add to the formula a term with m = 0 to fit the steady state strain portion of the creep curve.

$$S = Ct. \text{ where C is constant.} \qquad (10)$$

McVetty (22) has suggested that the general relationship between secondary creep rate and the applied stress varies as the hyperbolic sine of stress.

$$\dot{S} = D \sin h \rho$$

Since $\sin h\, \rho$ approaches $\exp \rho$ for large values of ρ the exponentional relationship found by Dushman, Dunbar, and Huthsteiner (5) which is shown below can be predicted from McVetty's relation at large values of stress. A thorough investigation of the tertiary stage is not available in the literature presumably for the reason that at this stage the material's ultimate failure is a certainity.

Dushman, Dunbar, and Huthsteiner (5) have shown that for polycrystalline materials at fairly high stresses the creep rate "$\dot{S}$" is related to the stress ρ and the absolute temperature T, by an equation of the form (5, p. 108):

$$\ln (S/T) = - a/T - b + \alpha \rho \qquad (11)$$

in which a and b are constants, and α is a function of temperature, but not of stress.

When the deformation reaches a constant rate, the creep may be related to the stress by the equation:

$$S = d \exp (\alpha \rho) \qquad (12)$$

Where d is a constant, and if temperature is held constant, α is also a constant. For tests which extend into this region, beyond the period of transient creep, $\dot{S}$ may be identified with Andrade's constant C.

Phenomenological Treatment. A number of authors have indicated that the empirical approach does not add enough to the basic understanding of the strain-time process and that the theoretical approach has too narrow an application for practical consideration. Hence an intermediate approach, i.e., the phenomenological approach has been applied.

In the field of rheology a number of phenomenological models have been postulated to explain the time-dependent deformation of materials under stress. Figure 9 illustrates the three basic rheo-

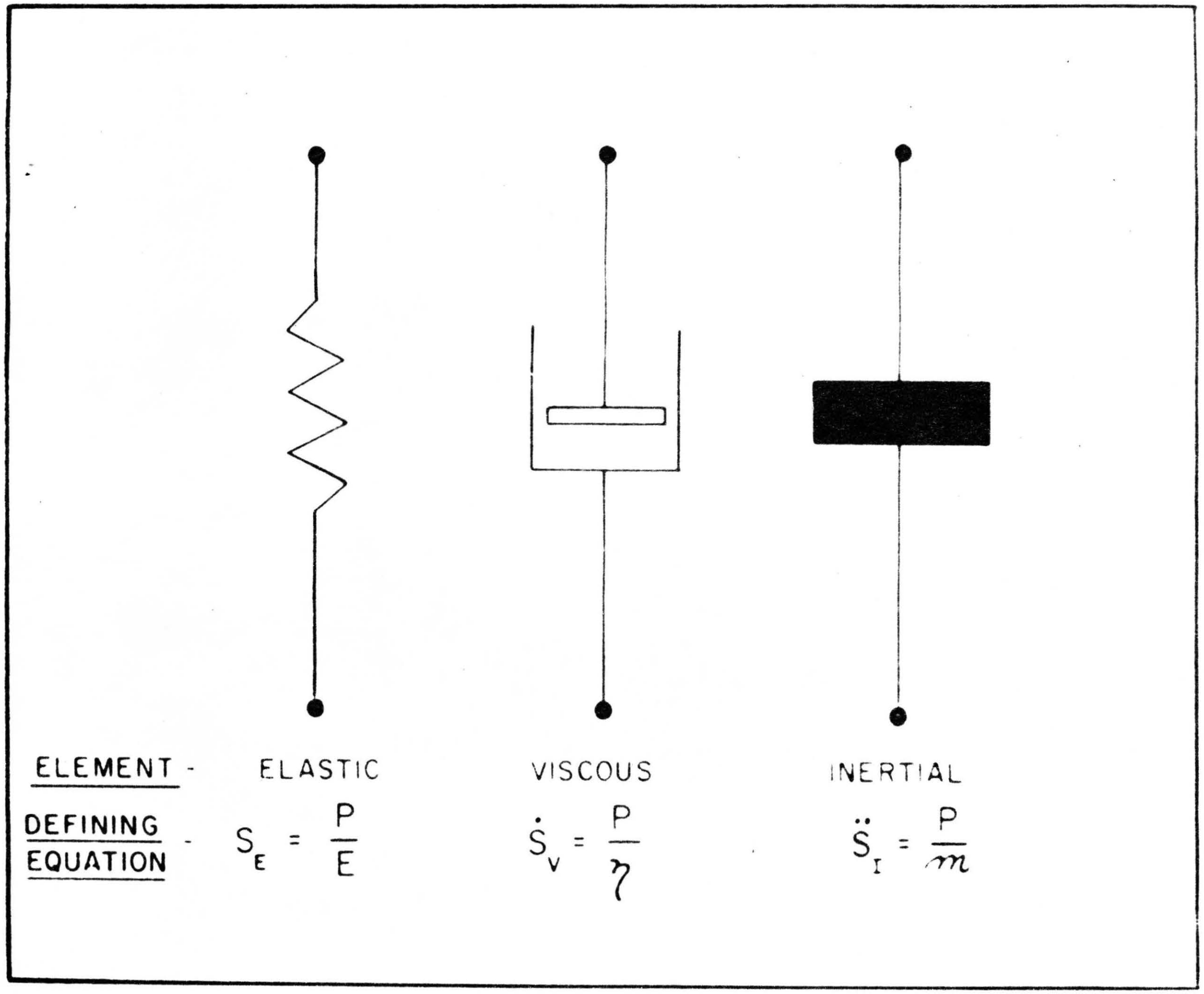

Figure 9. The basic rheological elements and their defining equations (After Hardy, 1959.)

logical elements and their defining equations. Burger (2) in reviewing the practical importance of these models, stated that the most important feature of the model system is the ability to adjust the arrangement of elastic and viscous elements, (in series or parallel), to duplicate the behavior of a particular metal. In the case of elastic and viscous elements in series, the elastic element may be neglected if a loading system of long duration is considered. The viscous element (piston) deforms continuously under every load resulting in a system which has an indefinite length, but can be extended or compressed at will. It is only in processes of short duration that the elasticity of the spring comes into play. The system consequently may be taken as representative of a fluid with a certain amount of instantaneous elasticity. In the case of an elastic and viscous element coupled parallel to each other, however, the behavior of the system is quite different. It is perfectly elastic under long term loads although its motions are retarded by an internal resistance depending upon the rate of load. For every value of load there is a definite final value of the extension. Such a behavior can be compared to that of an ordinary solid. If inertia is introduced into the model system, by replacing the points of application of the load by heavy masses, the system can describe damped oscillations similar to those in an ordinary solid body.

According to Burger, the deformation of certain materials which are often quoted as representative of cases where elastic and viscous effects occur simultaneously, can be explained by the behavior of more complicated rheological systems. The basic rheological model proposed by Burger consisted of a series combination of two basic units, the Maxwell unit (an elastic and viscous element in series) and a Kelvin or Voigt unit (an elastic and viscous element in parallel). Figure 10 illustrates Burger's model and the corresponding theoretical deformation-recovery curve.

For Burgers model, strain at any time is given by the following equation (2, p. 28):

$$S = (1/E_a + t/n_a + 1/E)(1-e^{-t/\zeta}) \qquad (13)$$

where $\zeta = n/E$, S is strain, P is the applied stress, t is the time after the application of stress, ζ is the retardation time (time necessary for the strain due to the last term to reach $\frac{1}{e}$ of its maximum value). E_a and E are the elastic constants and n_a and n are the viscous elements associated with the Maxwell and Kelvin units, respectively. The viscoelastic constants depend on the properties of the material under consideration.

It has been established that the above model definitely holds for coal Terry (30). Hardy (13) has shown that the model also applies to some types of rocks.

<u>Mechanisms of Creep</u>. In the field of metals and plastics a few people have tried to explain creep by the so called Dislocation Theory, which entails processes on an atomic or molecular scale. According to this theory the atoms in a slip plane cannot all slip simultaneously over their neighbors in the next plane; slip must begin at one place and then spread from there throughout the rest of the plane. The line within the slip plane which denotes the boundary of the slip front is called a 'dislocation'. When the atoms in the slipped region have

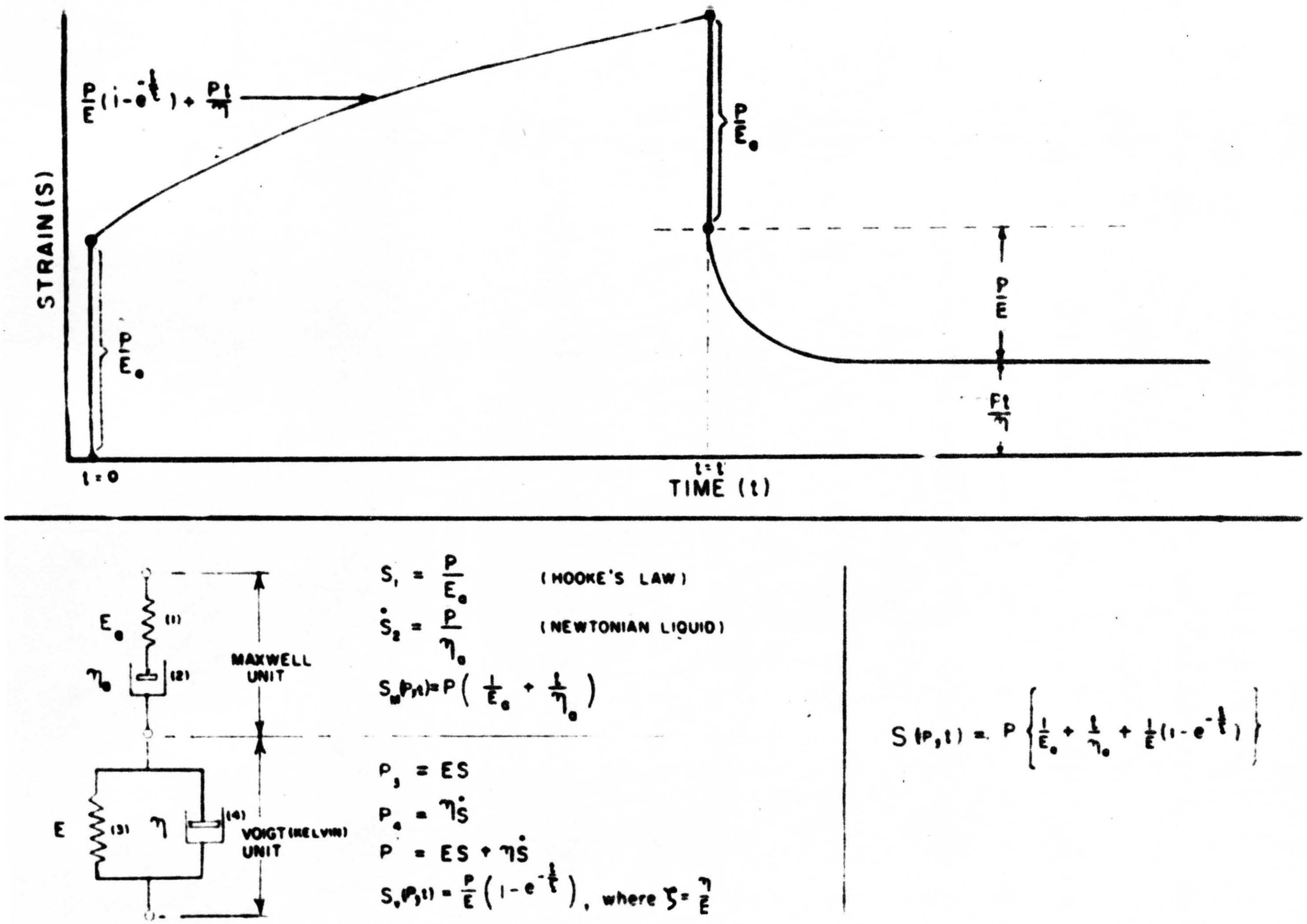

FIGURE 10. The Burgers rheological model. (After Hardy, 1959.)

moved by only one atomic spacing the slip front is called a unit dislocation (or, more often, simply a 'dislocation'). Slip fronts bounding regions of larger amounts of deformation are regarded as composed of many unit dislocations. A number of dislocations results in a change in length of the specimen. In certain instances, the movement and generation of dislocations in a body may continue over long periods of time if a static load is applied, resulting in creep. Transient and steady state creep have been explained successfully by this theory.

Creep in plastics has been explained by considering the untwisting of long molecular chains within the plastic structure. The relationship between applied stress and the resulting strain is similar to that given for metals in Equation 11.

It seems logical to apply these theoretical concepts to metals and minerals which bear a well defined structure, but in the case of rocks which are heterogeneous and anisotropic, the theoretical approach cannot be applied rigidly without making drastic assumptions.

Time-Dependent Deformation under Dynamic Loadings

Very little attention has been given to the effect of dynamic loads upon time-dependent deformation of materials, although it is well known that dynamic forces affect the behavior of materials and cause a reduction in their load resisting properties.

Creep of Geologic Materials.

There is very little information in the literature about time-dependent deformation in rocks due to dynamic loading. The only experimental data obtained to date was that of Terry (30, 32). He developed a composite oscillator method, using magnetostrictive excitation for the measurement of the internal damping of coal samples. The coal specimen in the form of a rod was cemented to a permendur transducer. The composite rod was sinusoidally excited, magnetostrictively, to mechanical resonance. His measurements covered a frequency range from 5 to 90 kc/s, and indicate that coal exhibits a frequency spectrum of retardation times. The retardation times increased rapidly as the frequency was decreased. It was concluded that coal behaves in a manner similar to that of a rheological model consisting of a chain of Voigt elements in series with a spring and dashpot.

Since this behavior could not be approximated by a simple Burger's model, a modified viscoelastic model having a Maxwell unit and i Kelvin units in series was utilized. The configuration of this model is shown in Figure 11. Using this concept with coal the strain at any time t is given by the equation (30, p. 319):

$$S = P\left(1/E_a + t/n_a + \sum_{i=1}^{N} \frac{1 - e^{-t/\zeta_i}}{E_i}\right) \qquad (14)$$

where $\zeta_i = n_i/E_i$, S is the strain, P is the applied stress, which may be a function of time, t is time after application of stress, ζ_i is the series of retardation times. E_a and E_i are the elastic elements and n_a and n_i are the viscous elements associated with the Maxwell and Kelvin units, respectively.

<u>Creep of Non-Geologic Materials</u>. Dynamic testing has been the object of intensive study where metals are concerned. However, most of the available material is either on the impact testing of metals or the fatigue aspect of a particular metal. There were a few instances where cyclic

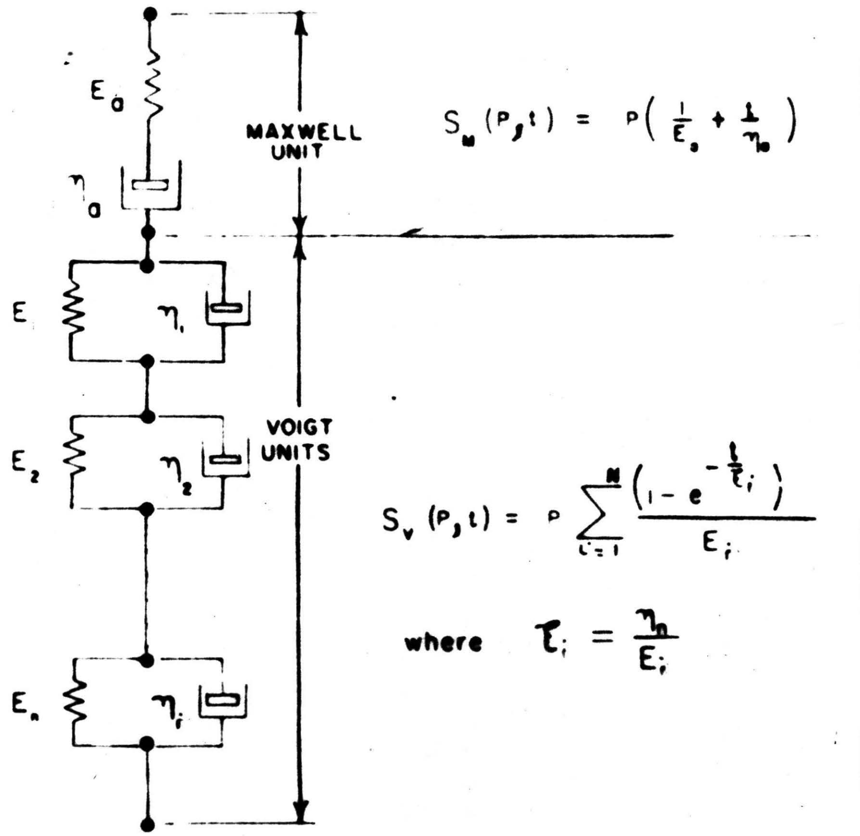

$$S_M(P,t) = P\left(\frac{1}{E_0} + \frac{t}{\eta_0}\right)$$

$$S_V(P,t) = P\sum_{i=1}^{N}\frac{\left(1 - e^{-\frac{t}{\tau_i}}\right)}{E_i}$$

$$\text{where } \tau_i = \frac{\eta_n}{E_i}$$

$$S(P,t) = P\left\{\frac{1}{E_0} + \frac{t}{\eta_0} + \sum_{i=1}^{N}\frac{\left(1 - e^{-\frac{t}{\tau_i}}\right)}{E_i}\right\}$$

FIGURE 11. The modified Burgers rheological model (with N different retardation times). (After Hardy, 1959.)

loadings on prestressed specimens were performed. There was no literature available pertaining to impact loads superimposed on prestressed metal specimens.

Impact Loading. Investigations by Mann (20) led to the statement that the work involved in producing deformation of a material depends on force, time, and space. The rate of deformation for maximum energy conversion depends on the composition and condition of the substance. He concluded that the dynamic properties of a material depend on three major factors; volume (determined using the length of the uniform least diameter or section), velocity of applied force, and material condition (influenced by temperature). McAdam and Clyne (21) found that the energy required in a single impact to produce fracture decreased very rapidly (in most steels) on passing a certain temperature, which was varied with the composition and heat treatment of the metal, the shape and size of the piece, and the speed of loading.

Investigations of Duwez and Clark (6) concerning the propagation of plastic deformation in metals under conditions of a longitudinal impact, showed that the phenomena observed can be explained by the Von Karman theory of plastic strain propagation. They concluded that this theory cannot be applied to materials for which the stress-strain curve has a continuously decreasing slope in the plastic range. Their experimental data indicated, in addition, that the relationship between stress and strain under impact conditions differs markedly from that under static conditions.

Campbell (3) established that in the case of a repeated direct impact within the elastic range, the relationship between impact velocity

V and the strain S', propagated into the specimen (3, p. 119), is:

$$S' = V/\sqrt{E_d/\rho} \qquad (15)$$

where ρ is the density of the specimen, and E_d is the dynamic modulus of elasticity. He observed experimentally that for impacts at low velocities, strains agreed well with those obtained from the theoretical expression. For the specimens of aluminum alloy tested, the results indicated that, within the conditions of the tests, the plastic strain caused by a given stress was considerably less than what would have been caused by that same stress applied statically.

Cyclic loading of pre-stressed specimens. Lazan (18) determined the effects of a superimposed sinusoidal cyclic stress on the creep of aluminum wire under static load, at room temperature. The tests were performed with a unidirectional cyclic tensile loading superimposed on a static tensile stress. His results indicated that low magnitude cyclic stress (peak to peak cyclic stress 59 percent of the static stress) caused a larger first stage total creep, an earlier commencement of second stage creep, and a lower second stage creep rate than was produced by a value of peak to peak dynamic stress twice that of the static stress.

Greenwood (7) found that sinusoidal vibration increases the rate of creep, and also accelerates recrystallization under constant stress in most metals, when the vibrations are superposed on a direct tensile stress. The observations of Poa and Marin (24) on a new four unit dynamic creep testing machine designed to work for low values of static loads are given in Figures 12 and 13. The static load in these tests was a tension applied by means of a lever arm, and the cyclic

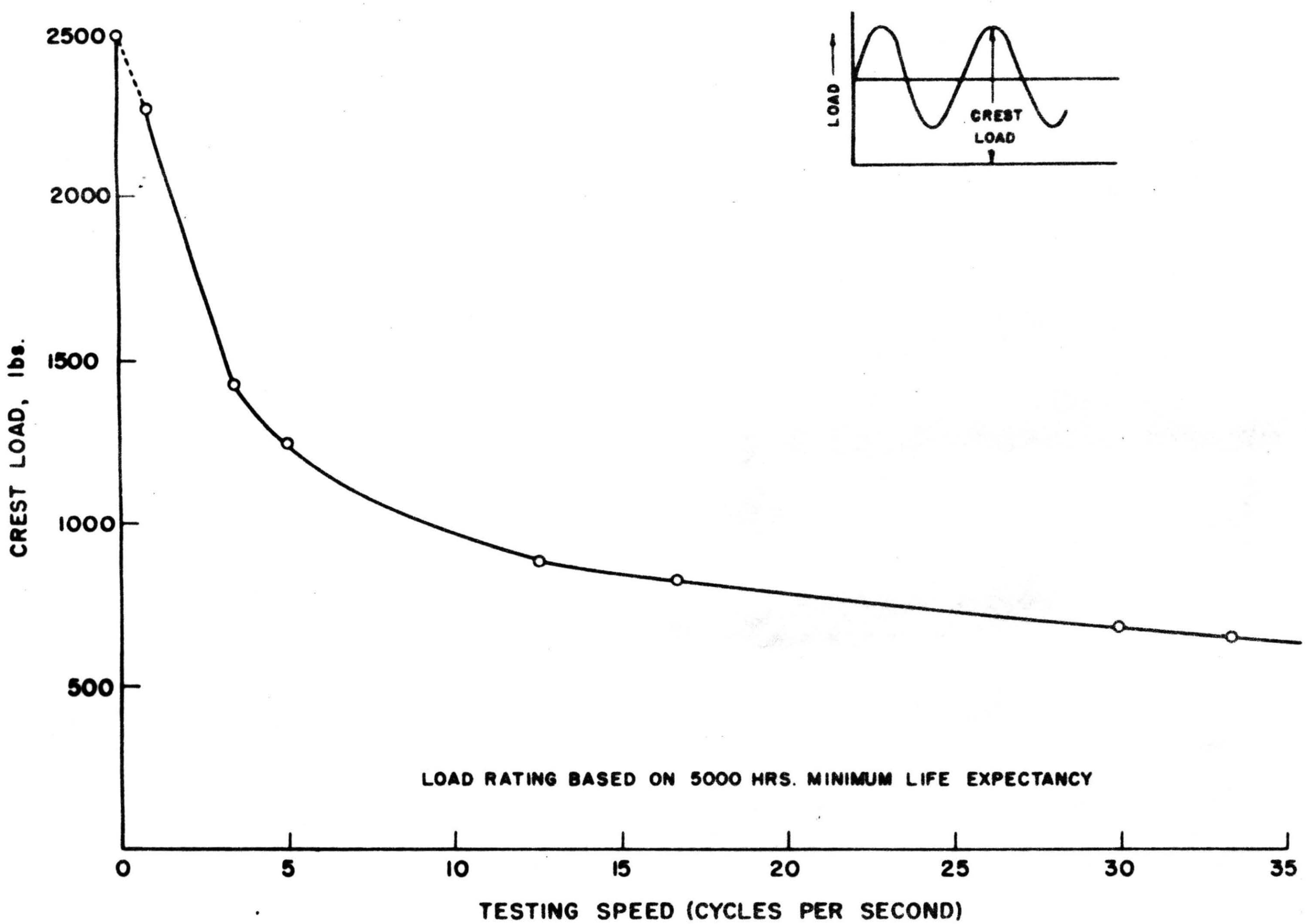

FIGURE 12. VARIATION OF ALLOWABLE CREST LOADS WITH TESTING SPEED. (After Poa and Marin, 1954.)

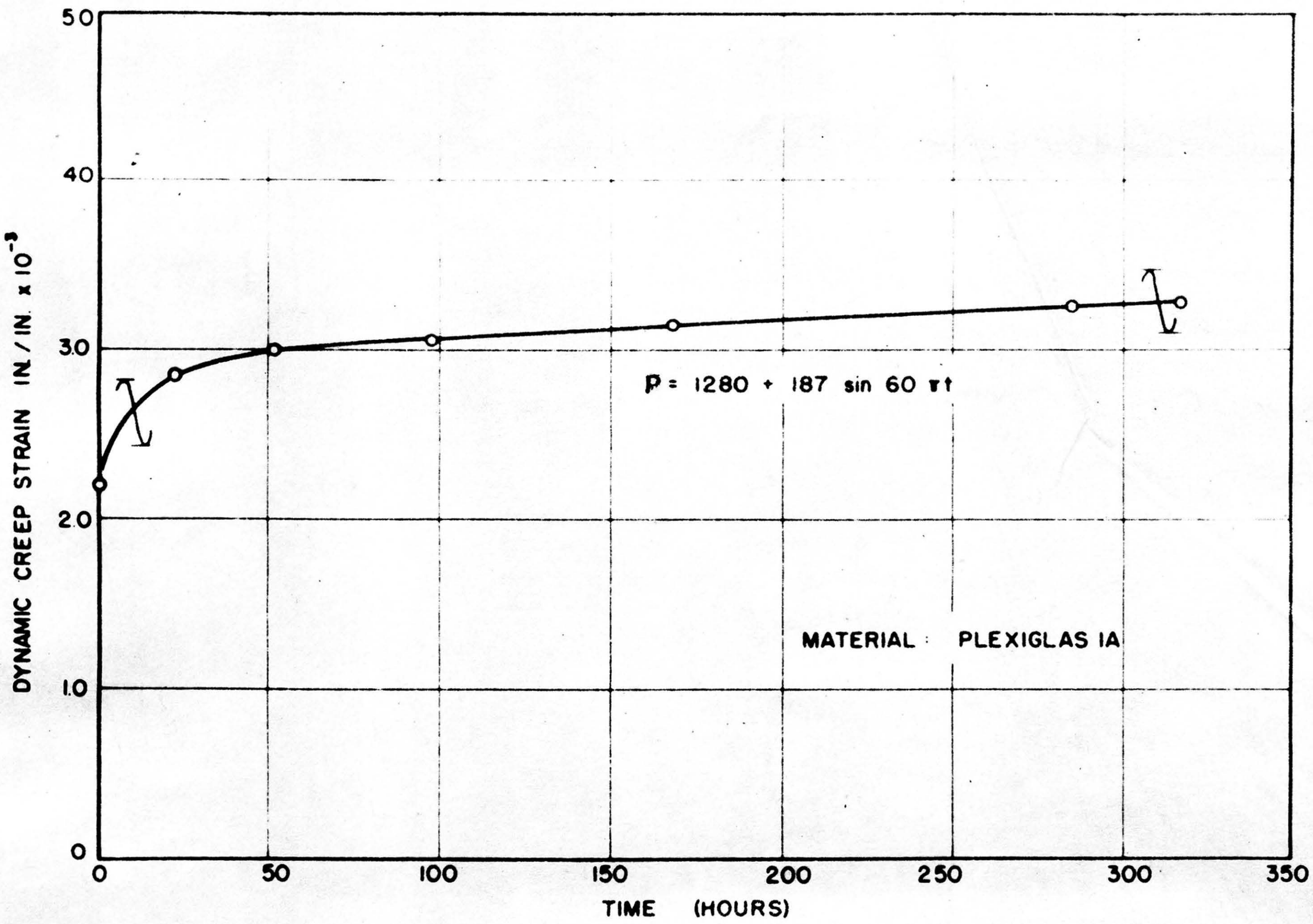

FIGURE 13. A TYPICAL DYNAMIC CREEP-TIME CURVE. (After Poa and Marin, 1954.)

load was obtained by means of an eccentric. Figure 12 shows the variation of crest loads, with testing speeds, to give a 5000 hour minimum life expectancy, a curve of the same general form as S-N curves used in fatigue life determination.

A typical dynamic creep-time curve for plexiglas obtained with a sinusoidal stress of 187 psi. peak magnitude oscillating at 30 cps, superimposed on a static stress of 1280 psi., is presented in Figure 13. This curve has the same shape as the creep-time curves obtained for materials under static load. (See Figure 6).

CHAPTER III

LABORATORY INVESTIGATION

The laboratory investigation consisted of the design of apparatus for static and dynamic loading of gypsum creep test specimens, and the development and application of creep test procedures.

Design of Apparatus

The investigation of the time-dependent behavior of gypsum rock under dynamic loads was complicated by the fact that there was no commercially available testing equipment to fit the specific test needs. Therefore, a considerable portion of the research time was involved in the design and testing of rock creep apparatus.

The design portion of this study consisted of three phases: (1) assembly of a static loading machine (2) construction of a dynamic loading unit, and (3) development of instrumentation for long term strain measurements.

Static Loading Machine

The first items constructed in the laboratory were equipment designed to apply long-term static loads to gypsum specimens. This was necessary due to the lack of information concerning the static creep properties of gypsum and the need for a basis for evaluating the effect of superimposed dynamic loads.

The static loading machine consisted of three, one-inch thick, mild steel, triangular plates; eight inches on a side. The three plates were inter-connected by three, ten-inch bolts of one-half inch diameter. The plates were free to slide along the bolts, relative to one another. A specially formed and calibrated spring was placed between the bottom and the middle plates. The specimen was placed between polished surfaces of the middle and top plates. The desired value of static loading was achieved by applying load with a hydraulic press to the top and bottom plates of the static loading machine, and then tightening the guide bolts to maintain the load. Figures 14 and 15, illustrate the components of a static loading machine and the use of the hydraulic press, respectively.

Dynamic Loading Unit

Two basic types of dynamic loading units have been used by investigators in the field of material creep; sinusoidal oscillators and repetitive-impact machines. The latter type units were not designed to apply dynamic loads superposed on static loads.

For the purpose of this study, it was felt that the use of a repetitive-impact type dynamic creep testing unit was most desirable since the long-term dynamic loads experienced by rock underground are most likely to be of an impact nature. The primary difference between this unit and those of previous investigators was the introduction of means of statically pre-loading the rock specimens.

The dynamic loading unit consisted of four modified static loading machines, each machine modified by machining a one and one-half inch diameter hole in the top plate. An anvil with a flat lower surface

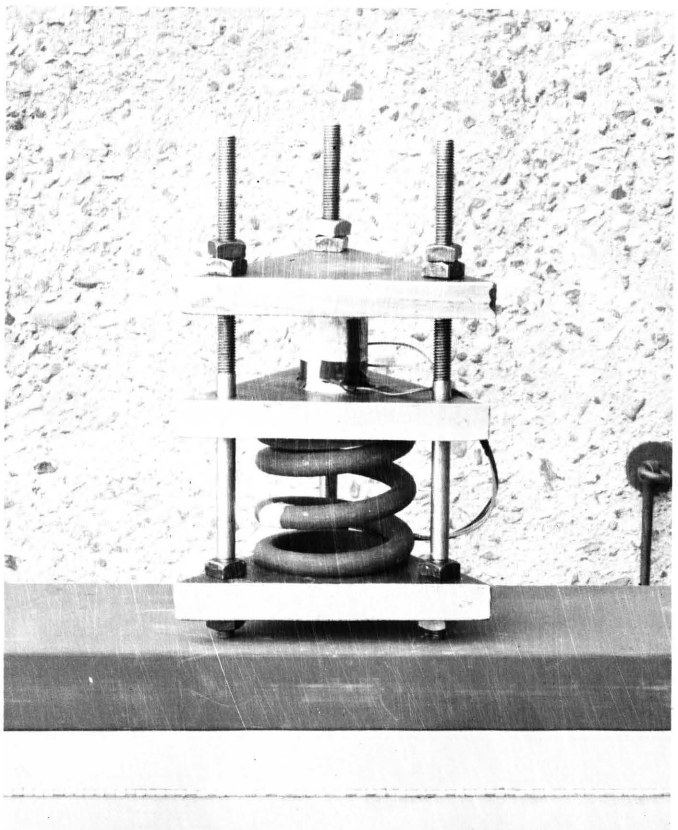

Figure 14. Static loading machine for creep tests of rock specimens.

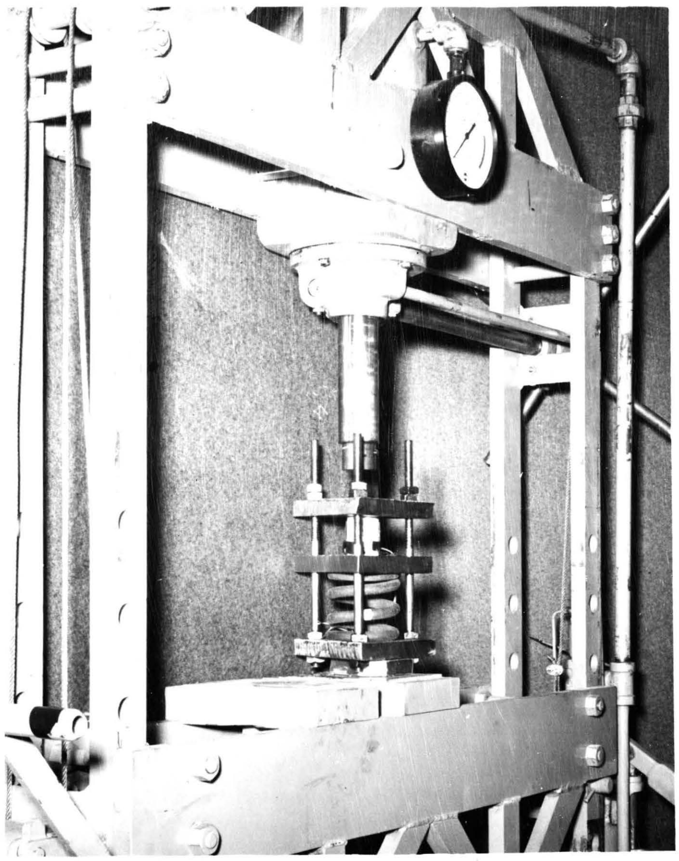

Figure 15. Hydraulic press used to develop a static preload.

was placed between the top of the specimen and the upper plate; the upper end of the anvil extended through, and about one-half inch above, the plate. The four loading machines were bolted to a rectangular, fiberboard enclosed, angle-iron framework which housed the drop-weight mechanism used to apply dynamic loads. The enclosure minimized the effects of change of temperature on the specimens. A single cycle of impact load consisted of lifting a drop-weight to a predetermined height by means of an electromagnet and then releasing the weight. The anvil in the loading machine served to transmit impact from the drop-weight to the specimen. Figure 16 illustrates one dynamic loading machine from the unit.

Linear motion of the electromagnet was obtained by running the magnet support cables over carrier pulleys down to bolts attached to the periphery of fourteen inch diameter, circular plates fixed at either end of a central shaft.

A single-phase, one-quarter horsepower, thirty-nine and two-tenths r.p.m. (39.2) motor was used to rotate the central shaft by means of a v-belt drive. A wide range of repetitive rates could be obtained by a change of pulley ratio. The height of drop of the masses was controlled by microswitches, actuated by adjustable contacts on the rotating circular plates. The height of the magnet from the top of the anvil at the lowest point in the cycle could be adjusted by a change in cable length. All four electromagnets used for the lifting of the weights were powered from a twelve volt rectifier unit assembled for this purpose. Figure 17 is a photograph of an electro-

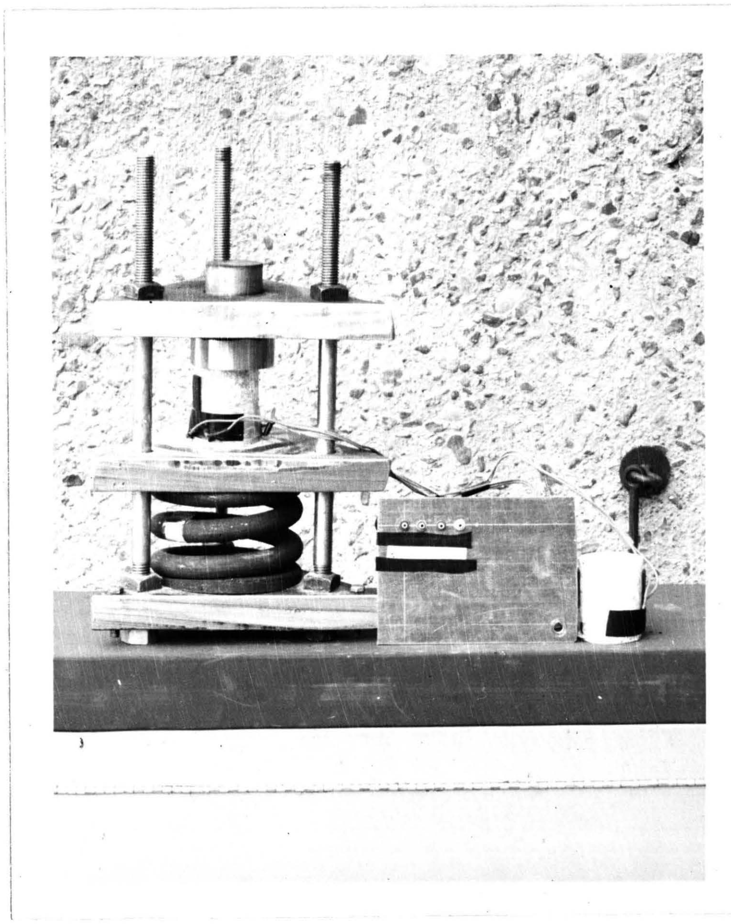

Figure 16. Dynamic loading machine developed to superimpose a repetitive impact load upon prestressed rock specimen.

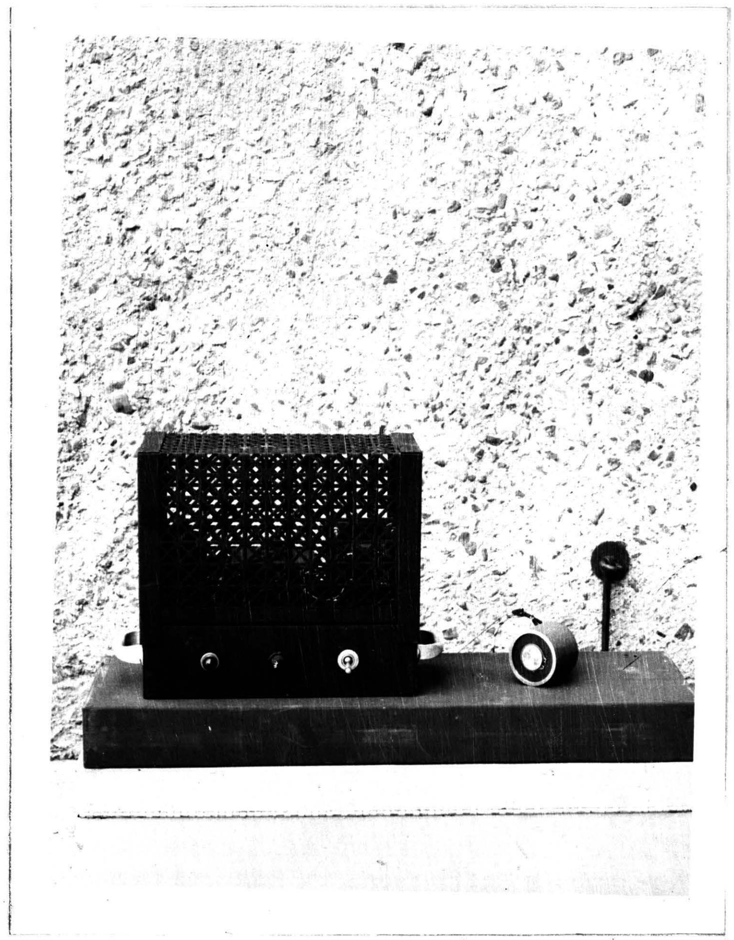

Figure 17. The 12 volt rectifier unit and the electromagnet for impact-mass suspension.

magnet and the power unit. Special drop-weights were made up to give impact to the specimen. They consisted of a one-tenth inch steel plate, underlain by a half-inch thick aluminum disc, beneath which was the remaining portion of steel stock needed to make up a particular weight. The purpose of adding the aluminum disc was to eliminate the effect of residual magnetism, and to achieve a controlled height of drop. Figure 18 shows some of the drop-weights used. Three masonite-surfaced angle iron guides served to align the drop-weight with the anvil. The complete dynamic loading unit assembly is shown in Figure 19.

Preparation of Specimens

The specimens used for the experimental study consisted of cylindrical sections of gypsum, one and one-fourth inches in diameter and two and one-eighth inches in length. The specimens were made from sections of core drilled from gypsum blocks in the laboratory, and after being cut to the right length with a diamond saw, were polished on both ends on a lapidary wheel. Two Baldwin SR-4, type A-3, strain gages were mounted vertically on each specimen. A special rapid setting Eastman 910 Contact cement was used for the application of the gages. It is claimed by the distributor, Tatnall Measuring Systems Company, that this cement has a very low creep rate for long time creep experiments. The surface of the specimen was roughened with sand paper and then cleaned thoroughly with acetone to increase adherance of the cement. An accelerator was applied to the strain gage paper and allowed to dry for half a minute under a dryer. Finally the

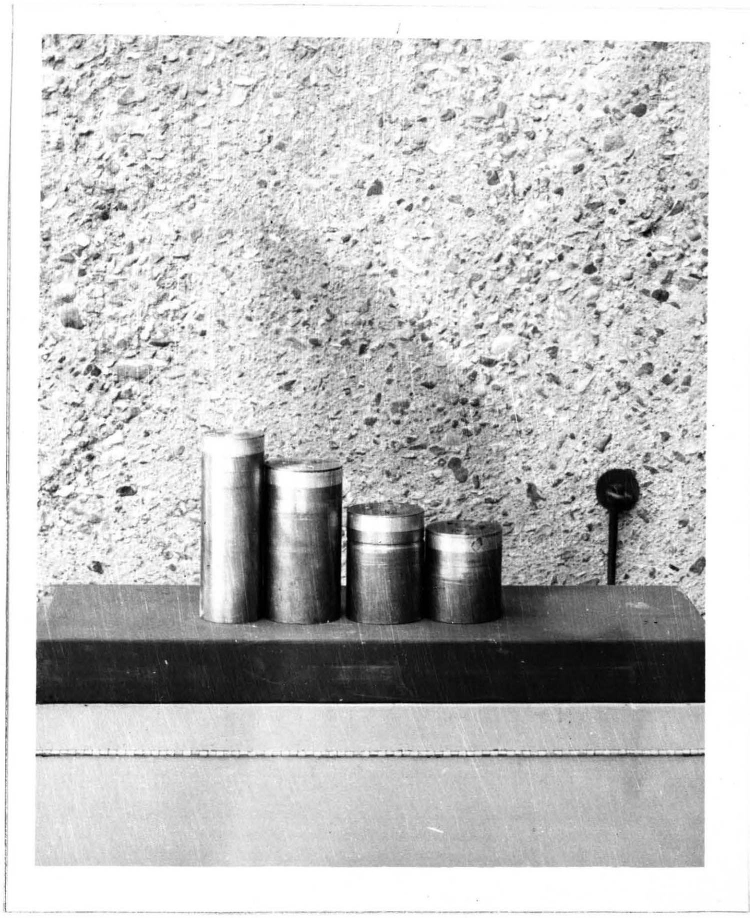

Figure 18. Drop weights used in the dynamic creep tests.

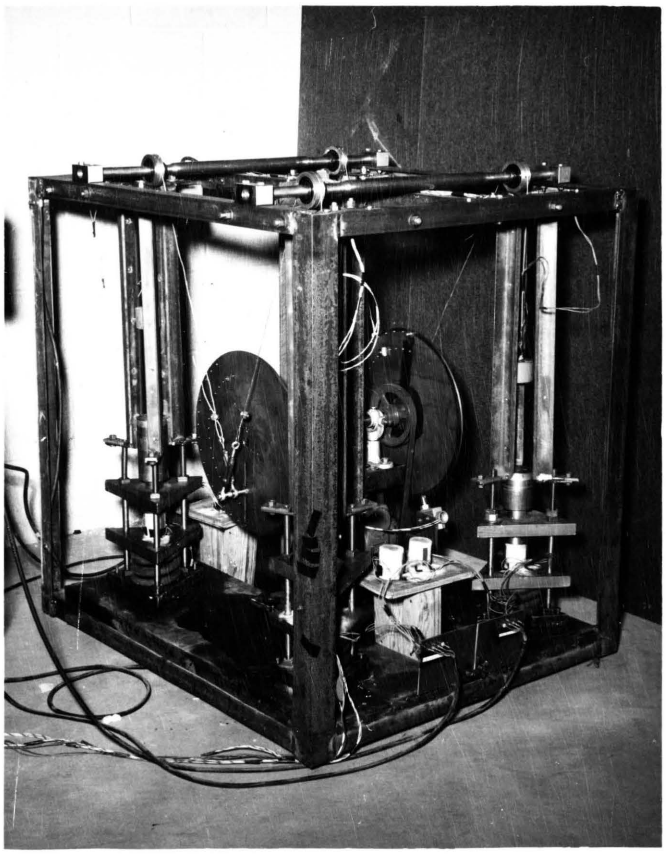

Figure 19. The complete four-unit dynamic loading machine.

rapid setting cement was applied and strain gage mounted. The strain gage was held in contact with the specimen for one minute, to give time for the cement to set. At the end of one minute, the cement was sufficiently hard to permit use of the specimen. There was no need for specimen aging.

Instrumentation

The measurement of creep behavior of materials is primarily a problem of accurately relating deformation to time. Time measurements must have greater precision during the first portion of a creep test than in the later stages. However, the use of a common pocket watch with a sweep second hand was found to be sufficiently accurate.

Deformations during creep tests have been determined in the past using spring loaded micrometers, dial-gauges, and electrical resistance-type strain gages. SR-4 strain gages were found to be most suitable for use in this investigation since (1) the overall change in length of the rock specimen during the test period was small, (2) strain gages were less likely to be damaged during dynamic tests, and (3) the disturbing influence of the heavy steel plates at the ends of the rock specimens on measurements was reduced to a minimum. SR-4 Type A-3 strain gages were used since the 13/16 inch nominal gage length was the longest which could be mounted satisfactorily, and the constantan wire grid used in the gage has a minimum sensitivity to variation in temperature.

A standard null-balancing strain gage bridge was used for measurements. The initial balancing controls were modified by addition of vernier dials to permit removal of the instrument for other tests, and re-use of the instrument without destroying the original balance condition.

Test Procedures

Static Test Procedure

A specimen, prepared as described previously, was placed in the static loading machine between the upper and middle plates. A specially manufactured spring, whose load-deflection characteristics had been determined previously in the testing laboratory, was placed between the lower and middle plates. A typical deflection-load curve for a spring from a static creep machine is given in Figure 23. The springs were designed to provide a maximum load of three thousand pounds. The entire machine was placed in the hydraulic press and compressed until the desired load was obtained; as indicated by a predetermined deflection of the spring. This deflection was held constant by tightening the nuts on the guide bolts.

Static creep tests were performed on gypsum specimens at compressive loads of 1500, 2000, 2500 and 3000 pounds, i.e., compressive stresses of 1330, 1770, 2220 and 2660 p.s.i., respectively.

Strain measurements required the use of active and dummy rock specimens to minimize temperature effects produced over a period of time. This is common practice in electrical strain gage measurements and requires no further explanation. It has been established that zero drift in strain readings due to the strain indicator instability has considerable effect over tests which extend over a long duration.

Figure 23. Typical Height-Load Curve for Static Preload Springs

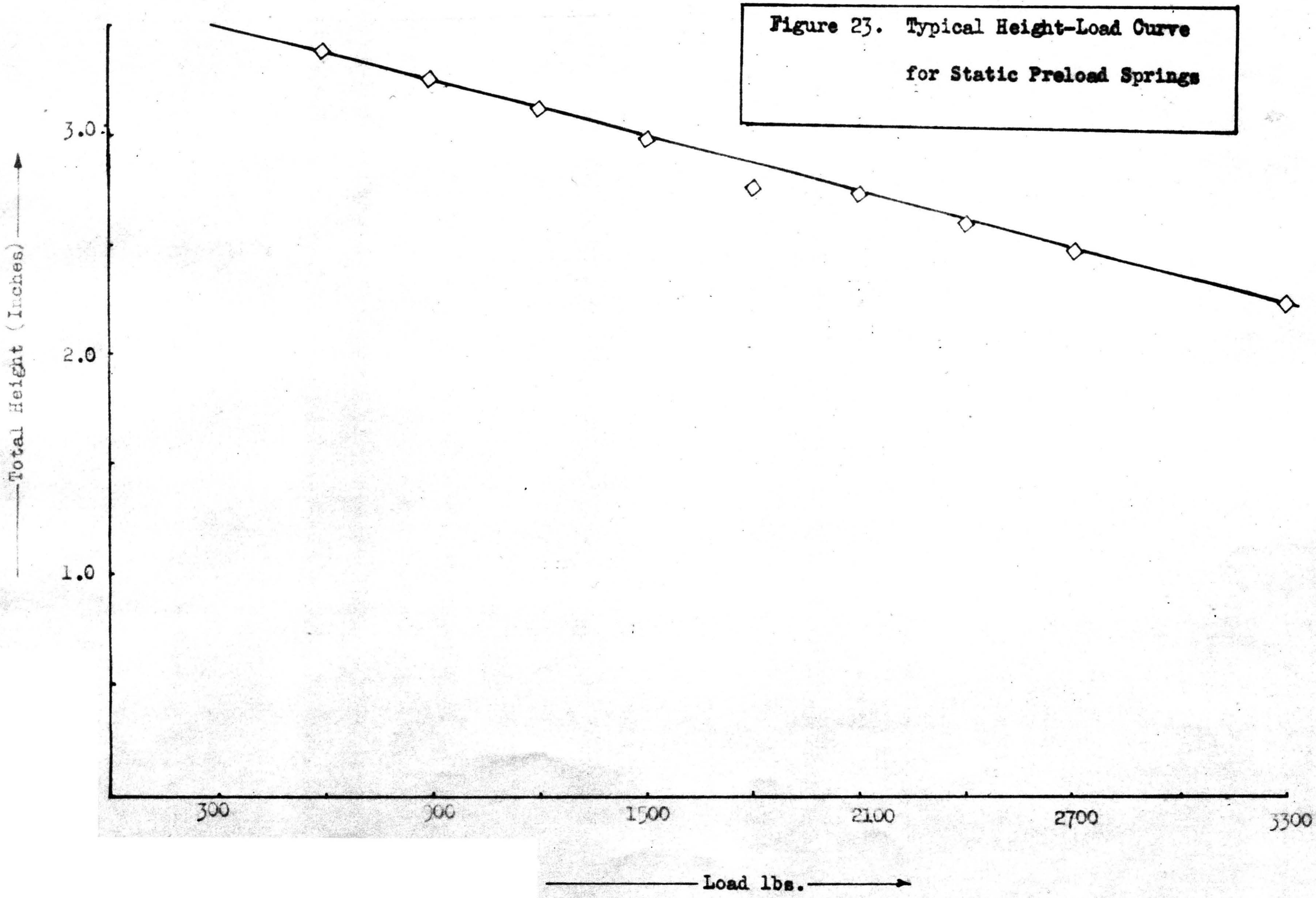

To eliminate this inaccuracy a modified wheatstone bridge circuit shown in Figure 20 was used. In examining effects of this circuit it was found that if strain gage R1 was strained in tension, its resistance would increase and the voltage at point A would drop slightly with respect to that at point C. It was apparent that if the positions of the active and dummy strain gages (R1 and R4) were reversed, this procedure would reverse the relative voltages at points A and C. However, the zero drift voltage due to indicator instability would not be reversed by this procedure, and therefore the strain indicated would be different in the reversed condition. Such a procedure would also reverse the sign of the apparent strain. Since the resistances of the active and dummy gages were not exactly equal, when the gage positions in the bridge circuit were reversed, the bridge null position at zero strain did not occur at the same setting of the balancing control. This caused the initial "normal" and "reversed" strain readings to differ, although in all cases, the indicating bridge was adjusted so that the initial normal reading was zero. A preliminary plot of normal and reversed readings of strain vs. time at measurement was made for the duration of test. The reversed strain curve was then adjusted to pass through the origin by removing the discrepancy between the initial reversed reading and zero, from every point on the original reversed strain curve. The median of the normal curve and the adjusted reversed curve was plotted, as shown in Figure 21. The true strain at any specified time was represented by the distance from the median curve to the normal curve.

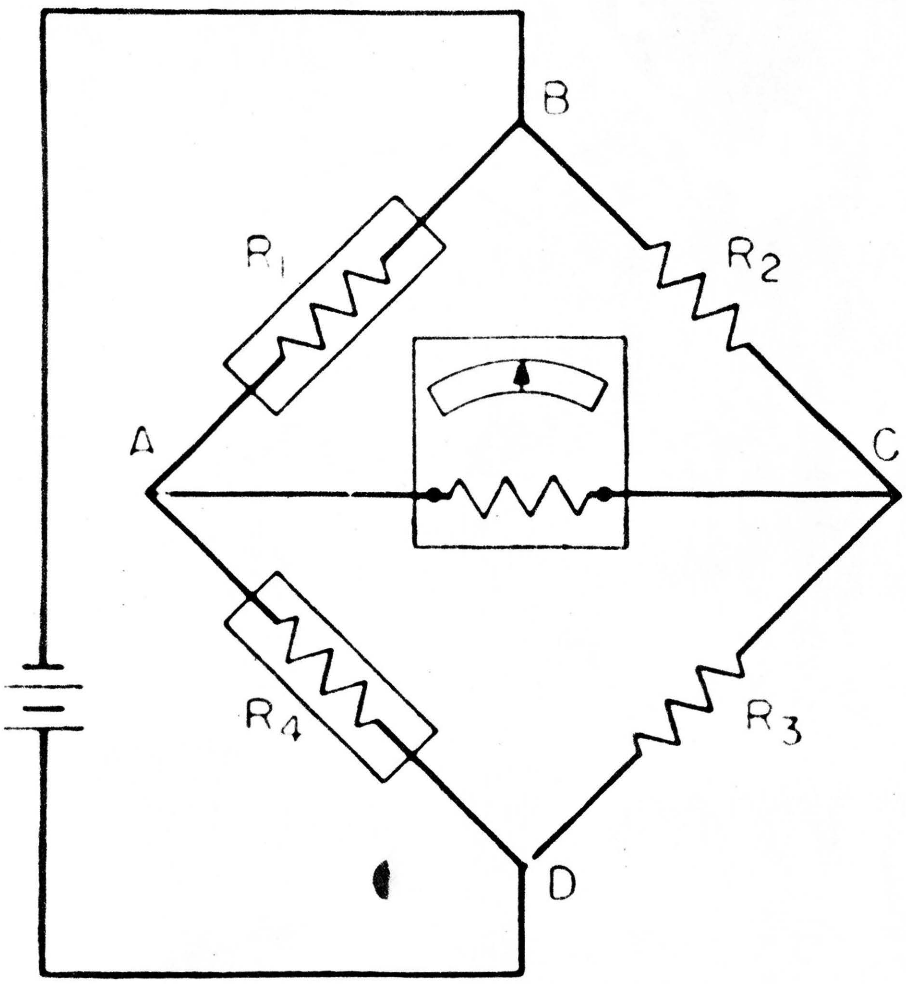

Figure 20. The modified wheatstone circuit used in long-term strain measurements with SR-4 strain gages.

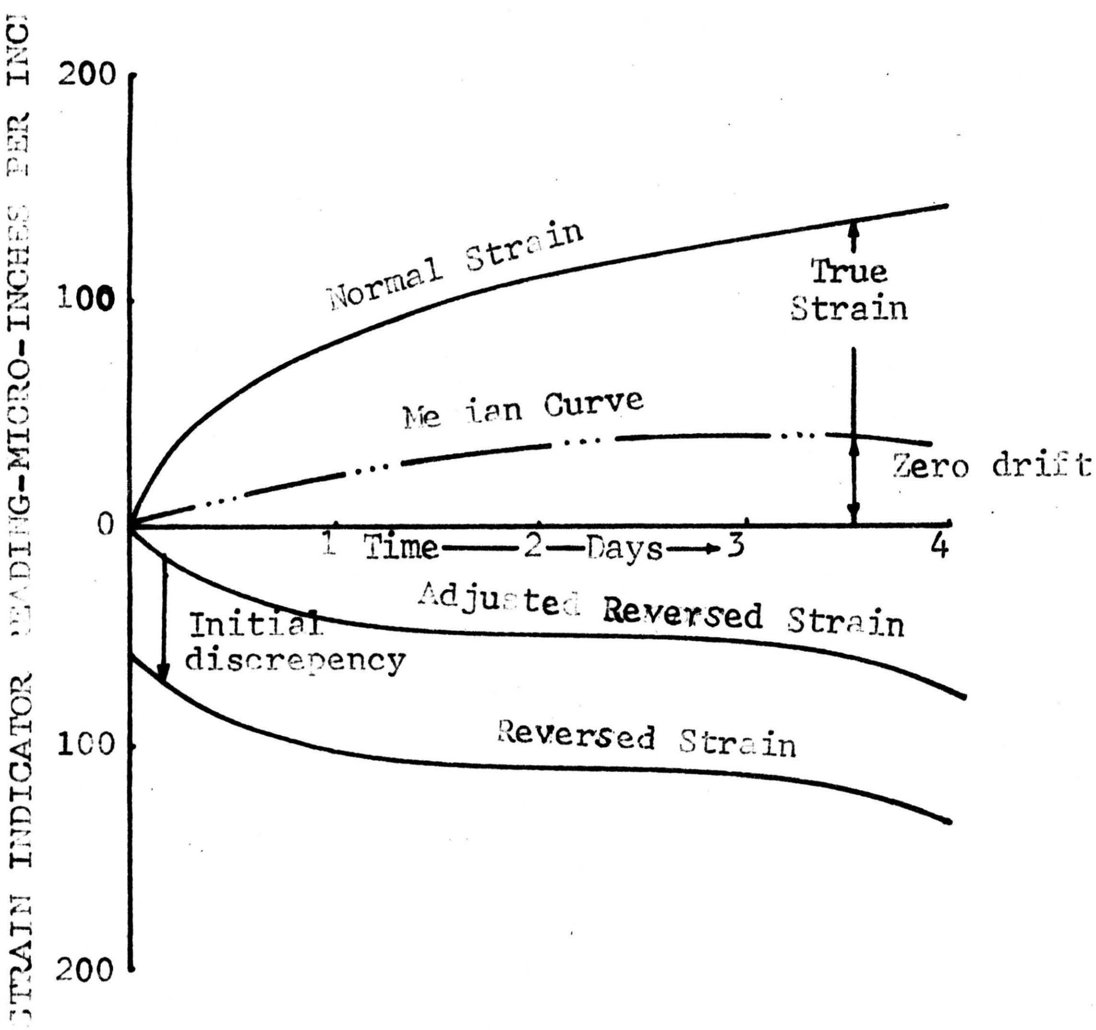

Figure 21. Typical strain reading illustrating zero drift and method of obtaining true strain.

Dynamic Test Procedure.

The dynamic test procedure consisted of two operations, namely, the loading of the specimen in the hydraulic press to obtain the desired value of static load, and application of dynamic load to the pre-stressed specimen.

The first step in the operation of the dynamic unit was adjustment of the height of release of the drop-weight through the micro-switch contact knobs. The modified static load machine was then placed in position, and bolted to the main frame, to reduce the adverse affects of vibration. The cable attached to the magnet was then adjusted to the proper length so that the magnet would just pick the drop-weight from the anvil. To assure consistent vertical drops, three guides were arranged around the impacting weight to maintain alignment of the weight with the machine anvil.

A repetitive impact test with 1500 lbs. of static preload, a 3.5 lbs. drop-weight, and a drop height of 4 inches was chosen as a basis of comparison for the series of impact tests which were performed. Strain measurements were obtained during each of the following series of tests, in which:

(1) Height of drop of the impact mass was varied from 2.0 to 4.0 inches, holding all other variables constant.

(2) Static load was varied from 1500 to 3000 lbs., holding all other variables constant.

(3) Drop-weight was varied from 2.5 to 5.0 lbs., holding all other variables constant.

(4) Combinations of weights and heights were selected which gave equal impact energies at a static load level of 1500 lbs.

(5) Combinations of weights and heights were selected which gave equal momentums at a static load level of 1500 lbs.

In dynamic testing of specimens, the same bridge circuit was used as in the case of the static tests, but reverse readings were not taken, since it was found that zero drift was negligible due to the construction of the strain indicator. The fact that the dynamic tests were of much shorter time duration than the static tests also reduced the importance of the effect of zero drift.

A no-load strain reading was taken before applying a static load to the specimen, and another reading of strain and time was taken after application of the static load. The dynamic loads were applied as soon as possible, and readings were continued at short intervals to determine the primary portion of the creep curve. Later, they were taken at increased time intervals as the creep curve approached the steady state portion. Figure 22 shows the RS-20C strain bridge with modified verniers adapted for rock creep research.

Analysis of Data

The same general procedure for data analysis was required in the case of both static and dynamic tests. Compressive strains were plotted versus time on both standard cartesian and semi-log coordinate paper. These curves were examined for any pronounced trends or

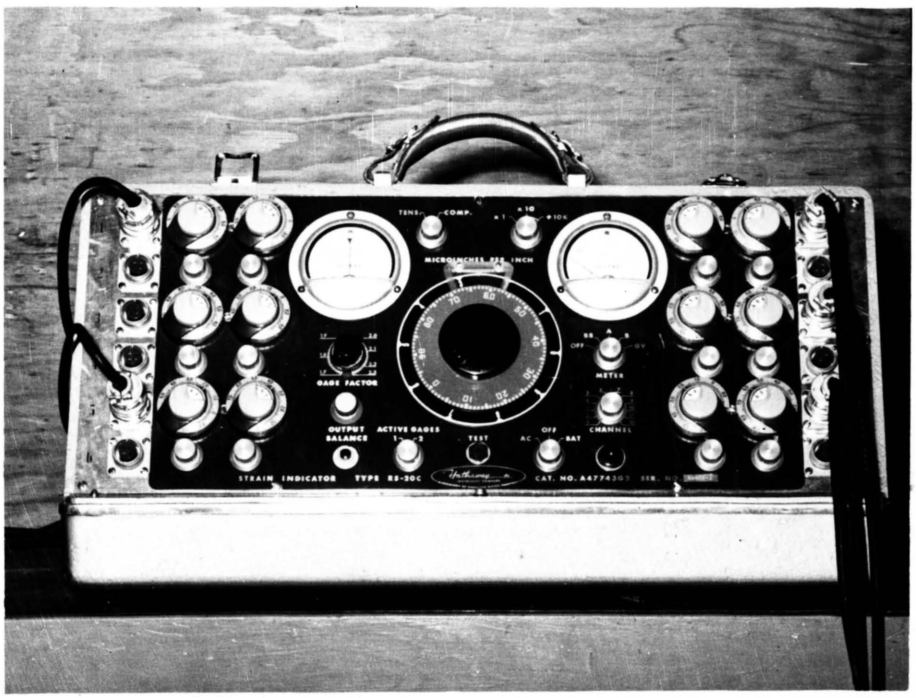

Figure 22. The Hathaway RS-20C portable strain indicator modified with vernier balancing dials, used with SR-4 type A-3 strain gages for creep measurements.

similarities. The coefficients of Grigg's equation for elastico-viscous deformation,

$$S = A + B \log t + Ct$$

were determined for static loading only. The coefficient A is equal to the strain at unit time, the coefficient B is equal to the slope of the semi-logarithmic strain curve at unit time, and the coefficient C is equal to the slope of the curve plotted on cartesian coordinates after a steady-state rate of strain was produced.

Static Creep Test Analysis

The coefficients a, b, c and d were determined from a variation of equation (13).

$$S = a + bt + c(1 - e^{-t/d})$$

Where the coefficient a is equal to the initial elastic strain (strain at zero time), b is the steady state rate of strain (slope of the straight line portion of the curve plotted on cartesian coordinates), c is the total elastic flow, and d is the retardation time. The method of obtaining these coefficients is illustrated in Figure 31. The results of the four tests under static loads of 1500, 2000, 2500 and 3000 lbs. have been presented in the form of strain-time curves on cartesian coordinates in Figure 24. Static tests were conducted with total loading times of ten days or more. The strain rate was constant after a period of 200 minutes, however, and therefore total time included in the figures was 1600 minutes.

The effect of change in static loading upon the coefficients A, B and C of Grigg's elastico-viscous equation is illustrated in Figure

32 (a). The coefficients a, b, c and d of equation (16) were also determined and are also presented in Figure 32 (b).

Dynamic Creep Test Analysis.

The dynamic test data is presented in a series of seven sets of related strain time curves.

The effect of a 3.5 lbs. drop-weight released from a height of 4 inches onto a specimen with 1500, 2000, and 3000 lbs. pre-load is indicated by three curves in Figure 25.

Strain-time curves for the condition of an impact mass of 3.5 lbs. and heights of drop of 2, 2.5 and 4 inches and a static load of 1500 lbs., are presented in Figure 26.

In the same manner, curves illustrating the effect of change in drop masses from 1.5 to 3.5 lbs. are presented in Figure 27. A static load of 1500 lbs. and a height-of-drop of 4 inches was maintained for this series.

One objective of the research was to determine whether the strain observed during dynamic creep tests was dependent upon impact momentum. For this reason, tests were performed with a constant 0.37 lb.-sec. (Fps-gravitational system) momentum at a static load of 1500 lb., for different combinations of drop weights and heights of drop.

To illustrate momentum-strain relations, curves for the following combinations of impact-drop-weight and height were plotted together: (1) 5 lbs. x 1 inch, (2) 2.5 lbs. x 4 inches, and 3.5 lbs. x 2.0 inches. This set is presented in Figure 28.

Another objective of this investigation was to find out, whether the strain observed during dynamic creep tests was dependent upon the drop mass impact energy. To achieve this objective, tests were performed with a constant impact energy of 10 in.-lbs.; holding the static load constant at 1500 lbs., for different combinations of drop weight and height of drop. The results are presented in Figure 29. The following combinations of weights and heights appear in these curves: (1) 2.5 lbs. x 4 inches; (2) 3.5 lbs. x 2.9 inches; and (3) 5.0 lbs. x 2.0 inches.

The steady-state strain rate portion of the dynamic strain-time curves was constant after a maximum time of 400 minutes. Data was presented in all cases for a test period of 1600 minutes.

In the literature review portion of this paper, reference was made to a study by J. D. Campbell, in which he determined that the relationship between static elastic strain and impact velocity in a static creep test of metals can be approximated by the theoretical relationship

$$S' = V/\sqrt{E_d/\rho}$$

The possibility of the application of this relationship to the gypsum time-deformation tests was of particular interest. The impact velocity for each of the tests performed was plotted versus the corresponding instantaneous impact strain, which was obtained by subtracting the initial static strain from the total elastic strain. This data is presented in Figure 30, together with a theoretical curve.

Curves showing the effect of variation of static preload, with a fixed magnitude of dynamic impact, upon the visco-elastic coefficients a, b, c, and d are shown in Figure 32 (c).

Variation of the visco-elastic constants with change in drop-weight and drop height, under a constant static preload, are plotted in Figures 33 (b) and 33 (c).

A second dynamic creep test was performed at a static pre-load level of 1500 lbs., and a dynamic impact level of 4 inch drop height and 3.5 lbs. drop weight to determine reproducibility of data. The results shown in Figure 34, show discrepancies much smaller than any of the variations due to changes in test parameters.

CHAPTER IV

CONCLUSIONS, RECOMMENDATIONS AND SUMMARY

Conclusions

Dynamic and static creep test data was obtained from more than thirty individual tests of a massive gypsum rock. The conclusions which follow are based on interpretation of this data, and are valid within the range of parameter variations included in the study. Certain of these conclusions may be applied to the more general field of creep testing, if some confirmatory tests are performed to define their limits of application.

1. Correlation of the static creep data obtained, with Grigg's and Burger's equations, equations (1) and (16), respectively, proved conclusively that Burger's equation describes the behavior of gypsum rock more accurately over the range of loading conditions obtained, than does that of Grigg's (See Figure 24).

2. Grigg's (9), tested alabaster, a fine-grained massive variety of gypsum, under a uniaxial static pressure of 1420 psi for a period of fourteen days. He determined the empirical relation between strain and time, $S = (13 + 6.5 \log t) \times 10^{-5}$, where t is in days.

The results of the present series of static tests on a massive gypsum rock indicated a much smaller elastic flow, on the order of $3.3 \log t \times 10^{-5}$, and a larger total amount of strain for a comparable stress level, 1330-1770 psi. (See Figure 32a).

The most logical explanation for this apparent discrepancy is that the gypsum rock used in the present series of tests was a heterogeneous material, and may therefore not be directly comparable to the alabaster tested by Griggs. The comparatively small creep strains were measured by Griggs using a dial indicator, whereas SR-4 strain gauges were used in the present study. It is felt that the use of strain gauges, resulted in a higher accuracy.

3. In the case of purely static loadings, it was found that the elastic portion of the curve, a, increased with an increase in load. Similarly the steady state rate of creep, b, increased with an increase in load, although not uniformly. Elastic flow, c, and the retardation time, d, remained approximately constant over all of the static load values investigated. (See Figures 24 and 32b).

4. The effect of an increase in static preload superimposed on a fixed dynamic load was to shift the steady state portion of the curve upwards as a result of an increase in the elastic flow portion, c, at a constant slope, b, and also to linearly increase the initial elastic strain, a, to a small degree. In contrast, the retardation time decreased with an increase in load. (See Figures 25 and 32c).

5. Increasing the height of drop (while holding all other parameters constant) not only increased the total elastic flow, c, considerably but also resulted in a linear increase in the initial

elastic strain, a. The retardation time, d, increased proportionally with drop height. It was seen that with an increase in the height of drop an increase in steady state creep rate, b, was very marked, although at greater heights of drop, this increase was less apparent. (See Figures 26 and 33a).

6. Equal impact energy, achieved with various combinations of drop weight and height, produced different strain levels as is apparent from Figure 29. Therefore, it appears that there is no correlation between impact energy and time-dependent strain. (See Figure 29).

7. It was found that equal momentum, achieved with various combinations of drop weight and height, produced approximately equivalent time-strain curves. This constant behavior is interpreted as evidence that the strain of the gypsum rock tested was a function of the impact momentum applied during the dynamic creep tests. (See Figure 28).

8. The curves drawn showing the effect of an increase in drop weight on strain, holding all other parameters constant, showed an increase in the slope, b, of their steady state portion as the drop weights were increased. The elastic strain, a, the maximum elastic flow, c, and the retardation time, d, also increased with increase in dynamic loads, the increase became more pronounced as the weights increased. (See Figures 27 and 33b).

9. An attempt was made to determine if any relation between impact velocity and dynamic strain in gypsum rock exists, as has been mentioned previously in the review of literature, in the case of metals,

where no static preload was applied. The results obtained were inconclusive. A trend can be seen in the data. However, there is insufficient data for any specific conclusion. (See Figure 30).

In summarizing the conclusions from these experiments, the most significant finding was that the time-dependent strain of the statically pre-loaded gypsum rock tested was a function of the impact momentum over the range of dynamic loads applied. The author feels that this relationship may be extended to other rock types and other dynamic loading conditions.

Recommendations

The writer would like to make a few recommendations as to the improvement of the mechanical set-up of the dynamic testing machine and for the facility of future investigations.

It was found that spring loading was sufficiently accurate for materials having a low creep rate and a low modulus of elasticity, but it is felt that a hydraulic loading system could give higher and more constant loadings than a spring where it is necessary to increase the scope of testing. This would also decrease the amount of time spent in fixing the loading machines to the dynamic unit.

Environmental control is essential for maximum accuracy. It is recommended that the unit be placed in a temperature and humidity controlled room if the length of the experiments exceeds thirty hours.

Adjustment of the height of drop could be more conveniently achieved by making a continuous slit in the adjusting portion of the rotating plates.

It was observed that the velocity of impact was of considerable importance in analysis of creep behavior. For the purpose of this investigation, velocity was calculated from the drop height, but it would be well worth the effort if it could be determined by measuring the time of travel experimentally between two fixed points on the guides.

It is recommended that an oscilloscope with a slow sweep be used to measure the dynamic strains produced in the form of a continuous record. The use of the oscilloscope would greatly facilitate analysis of the behavior of the specimen at the point of fracture.

The range of the dynamic creep test parameter should be increased, and other geologic materials should be tested to determine the validity of extrapolation of the results obtained in this study.

A study should be made of the effect of rate of repetition of impact upon the time-dependent strain.

An investigation of the effect of different forms of dynamic loads, sinusoidal, impact, etc., on geologic materials should be conducted.

Summary

A static loading machine and a four unit dynamic loading creep testing unit was designed and assembled. Static tests were performed as a means of calibration of the gypsum rock tested. The dynamic unit was used to apply an impact to prestressed gypsum specimens with different combinations of drop weights, drop heights, and static preload levels. The impact was applied by the use of aluminum shielded, mild steel, weights which were picked up by electromagnets. Gypsum specimens of 1 1/4" diameter and 2 1/4" length were used throughout the experiments. Laboratory measurements of dynamic strain were achieved by use of a modified strain indicator, using a temperature compensating Wheatstone bridge circuit.

Investigations were performed to determine the effects of static load alone, the effect of fixed dynamic load superimposed on different levels of static load, the effects of different drop heights and masses, the effect of equal impact momentum and energy, and the relation between impact velocity and elastic dynamic strain.

This data was plotted on the cartesian coordinates and using equations which had been derived phenomenologically, visco-elastic coefficients were determined empirically. The investigation led to the conclusion that for the particular gypsum rock tested within the elastic limit of the material, time-dependent strain is a function of impact momentum. An increase in the momentum would result in a proportional increase in strain.

APPENDIX

A. Compilation of Creep Test Data

B. Geologic Description of Gypsum Specimens

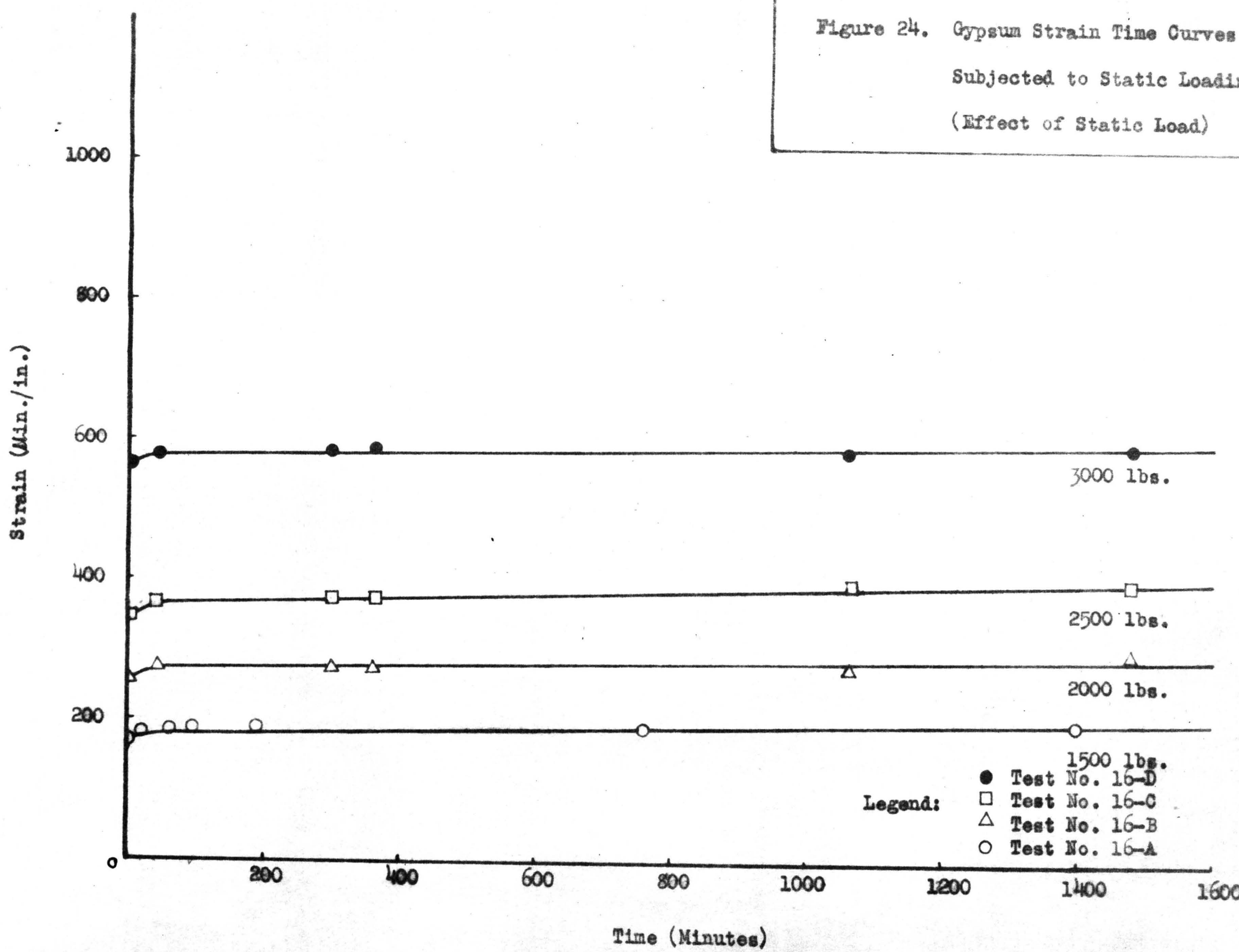

Figure 24. Gypsum Strain Time Curves Subjected to Static Loadings (Effect of Static Load)

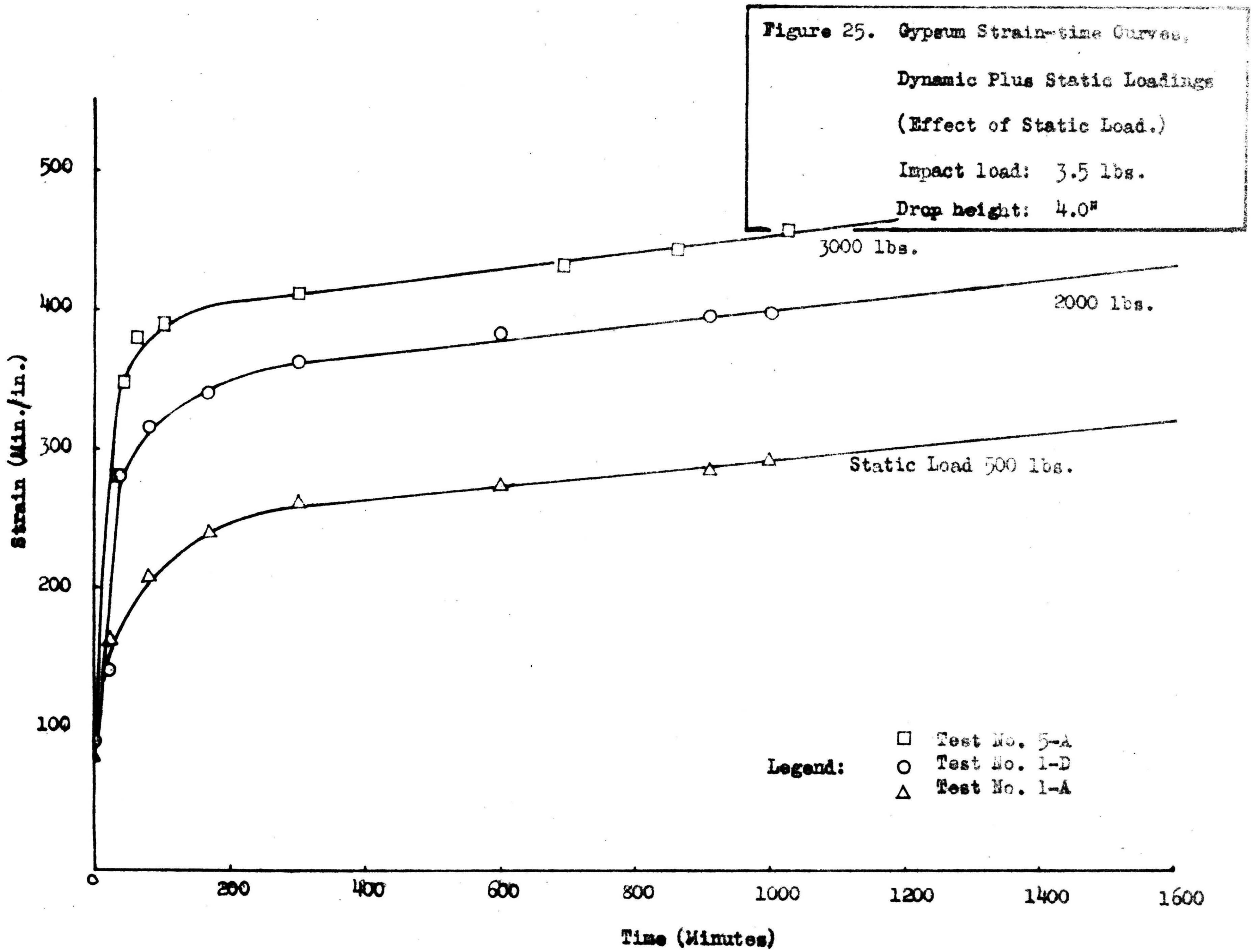
Figure 25. Gypsum Strain-time Curves,
Dynamic Plus Static Loadings
(Effect of Static Load.)
Impact load: 3.5 lbs.
Drop height: 4.0"
3000 lbs.
2000 lbs.
Static Load 500 lbs.
Strain (Min./in.)
500
400
300
200
100
0
200
400
600
800
1000
1200
1400
1600
Time (Minutes)
Legend:
Test No. 5-A
Test No. 1-D
Test No. 1-A

Figure 26. Gypsum Strain-time Curves,
Dynamic Plus Static Loadings
(Effect of Drop Height)
Impact load = 3.5 lbs.;
Static load = 1500 lbs.

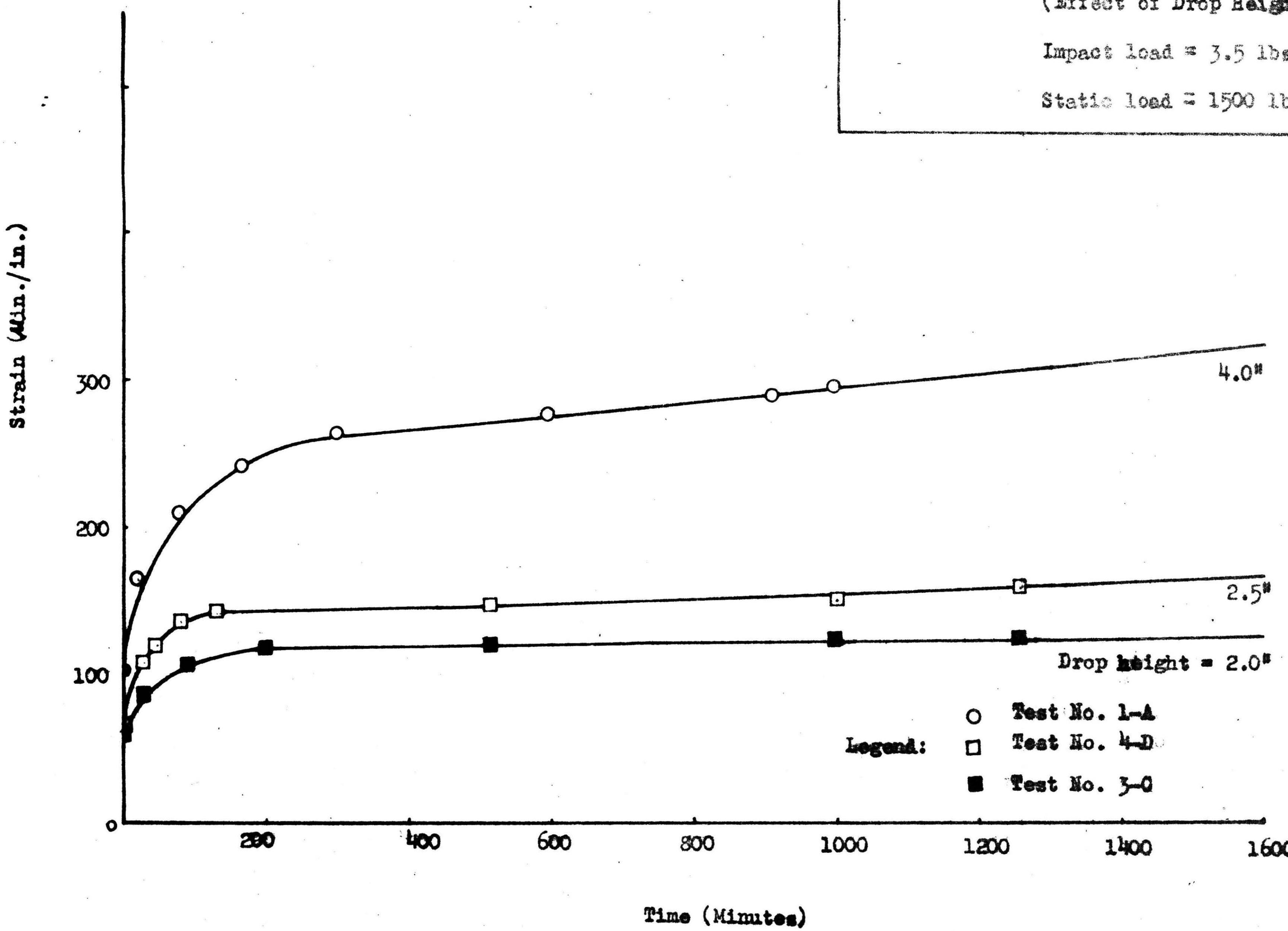

Figure 27. Gypsum Strain-time Curves, Dynamic Plus Static Loadings (Effect of Drop Weight) Height of drop = 4.0"; Static load = 1500 lbs.

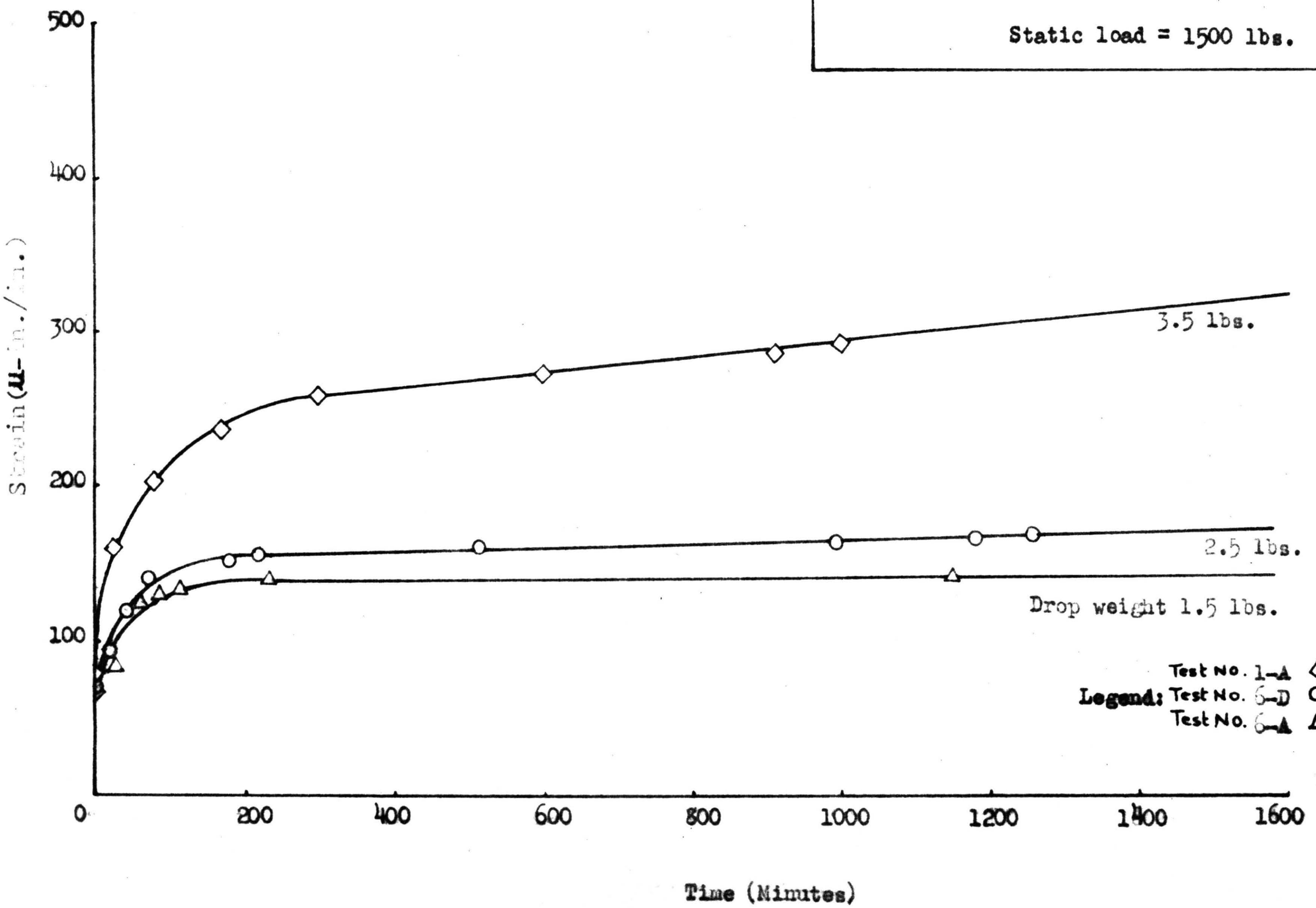

Figure 28. Gypsum Strain-time Curves, Dynamic Plus Static Loadings (Effect of Equal Momentum) Static load= 1500 lbs

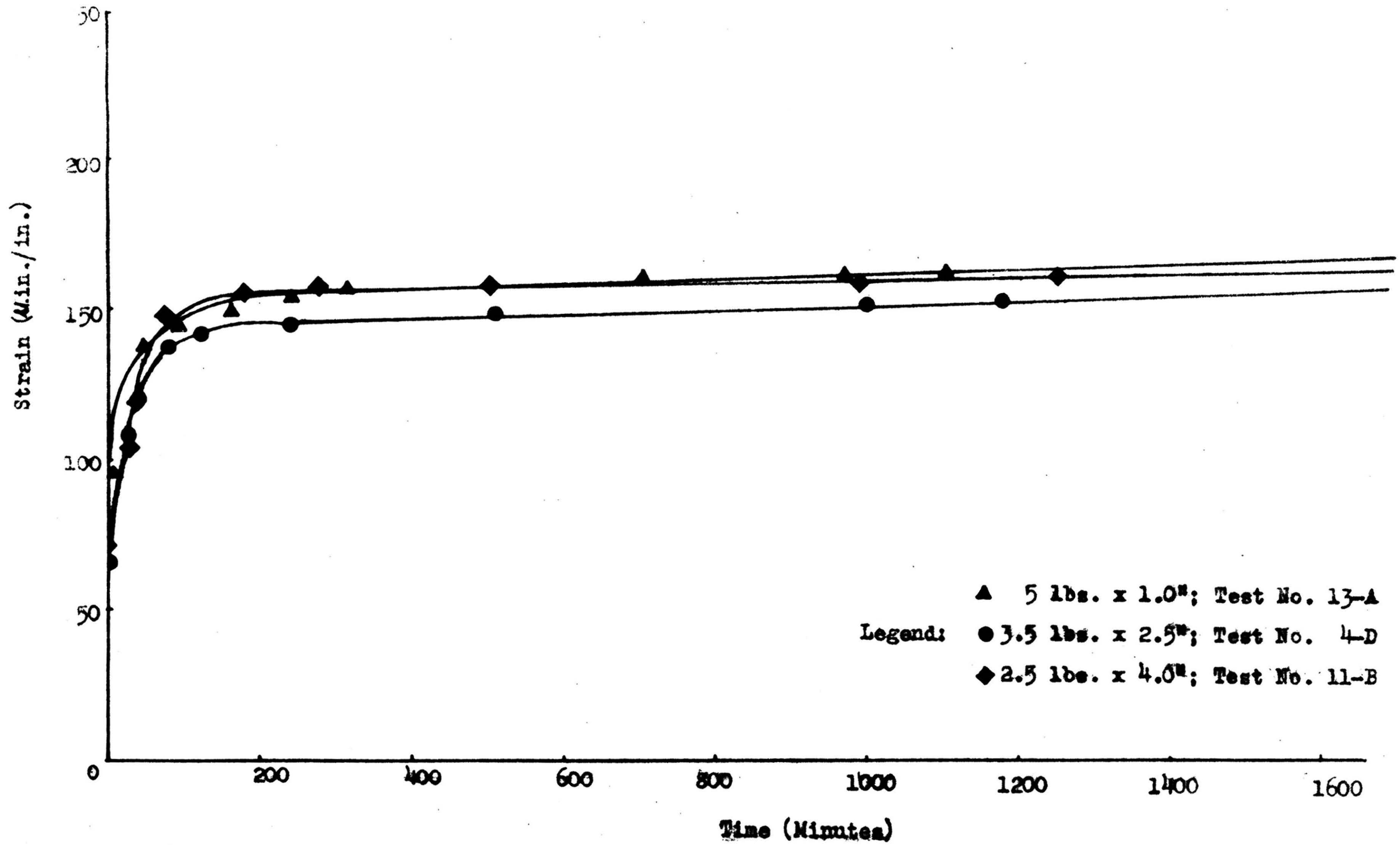

Figure 29. Gypsum Strain-time Curves, Dynamic Plus Static Loadings. (Effect of Equal Impact Energy) Static Load = 1500 lbs.

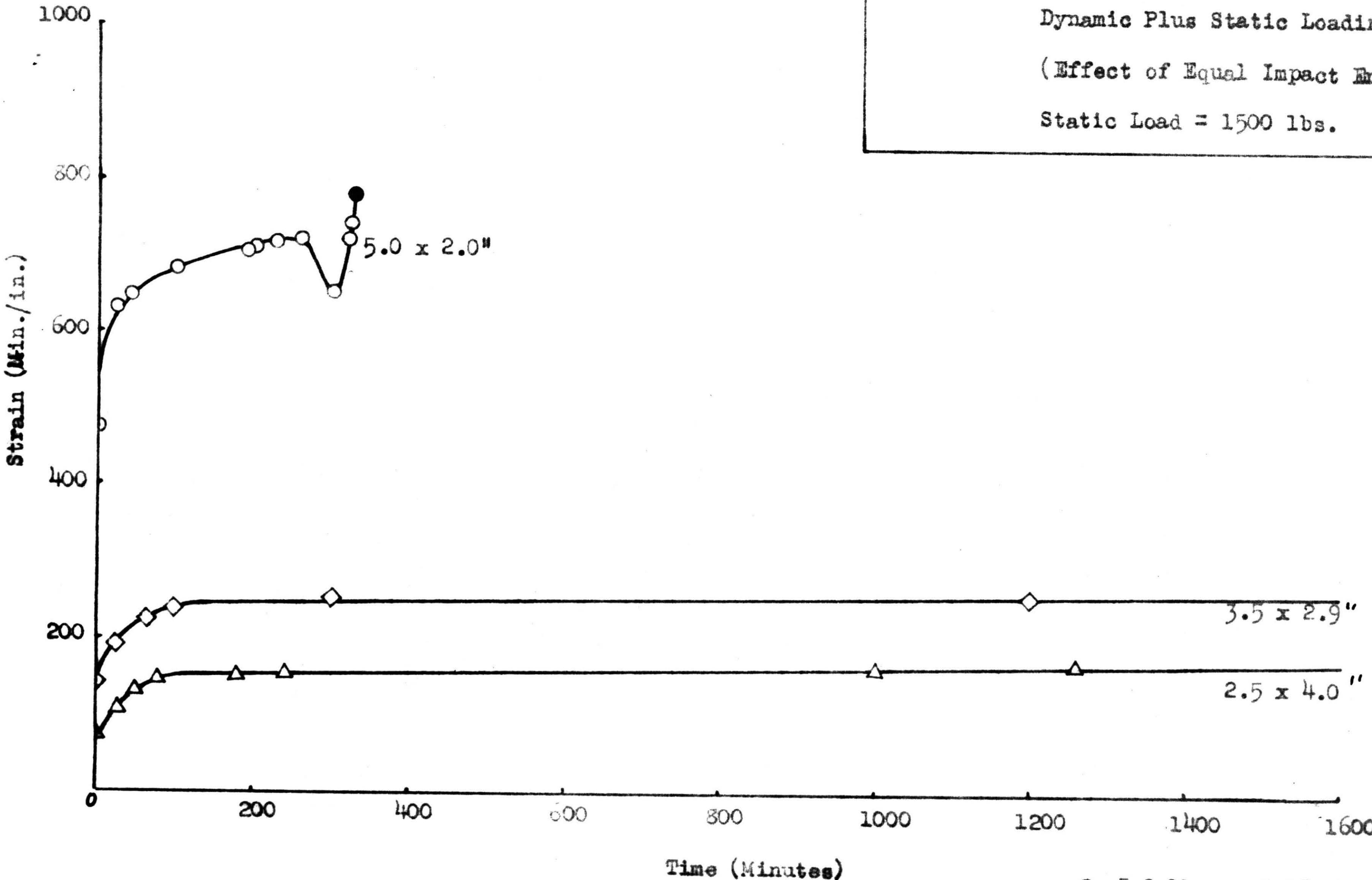

Legend:
○ 5.0 lbs. x 2.0"; Test No. 9-C.
◇ 3.5 lbs. x 2.9"; Test No. 9-A.
△ 2.5 lbs. x 4.0"; Test No. 6-D.

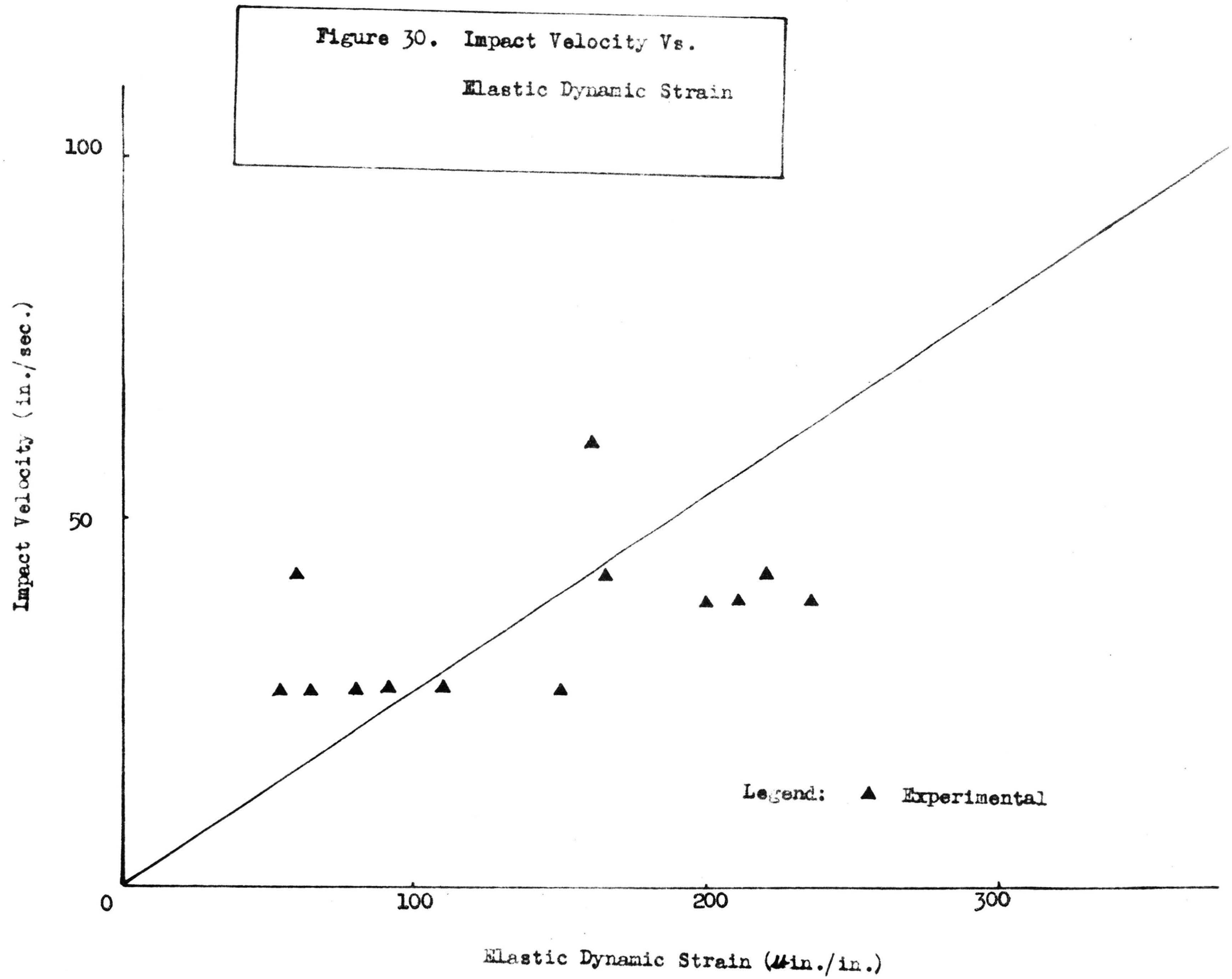
Figure 30. Impact Velocity Vs.
Elastic Dynamic Strain
100
50
0
Impact Velocity (in./sec.)
100
200
300
Elastic Dynamic Strain (μin./in.)
Legend: ▲ Experimental

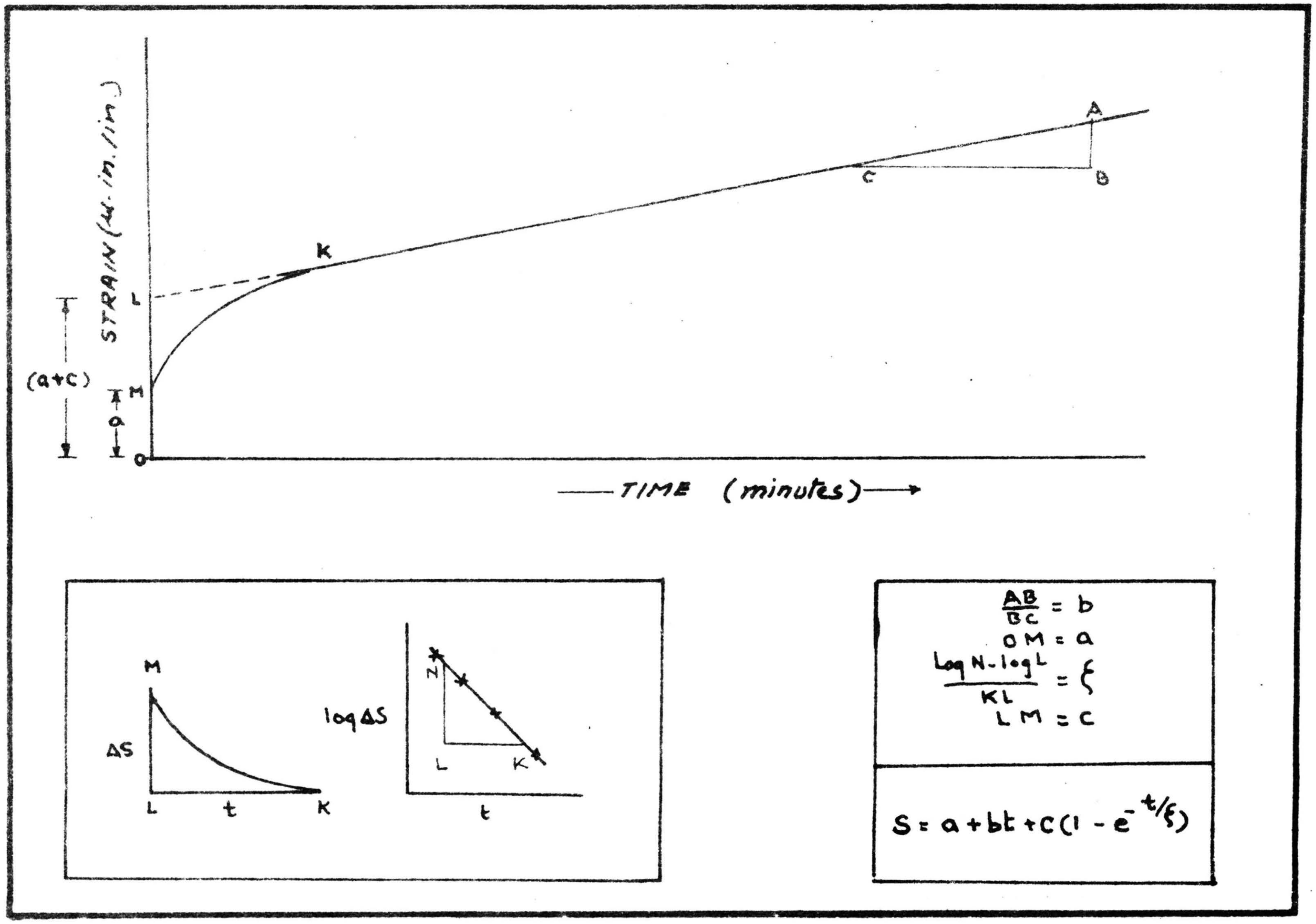

Figure 31. Graphical Determination of Elastico-Viscous Coefficients

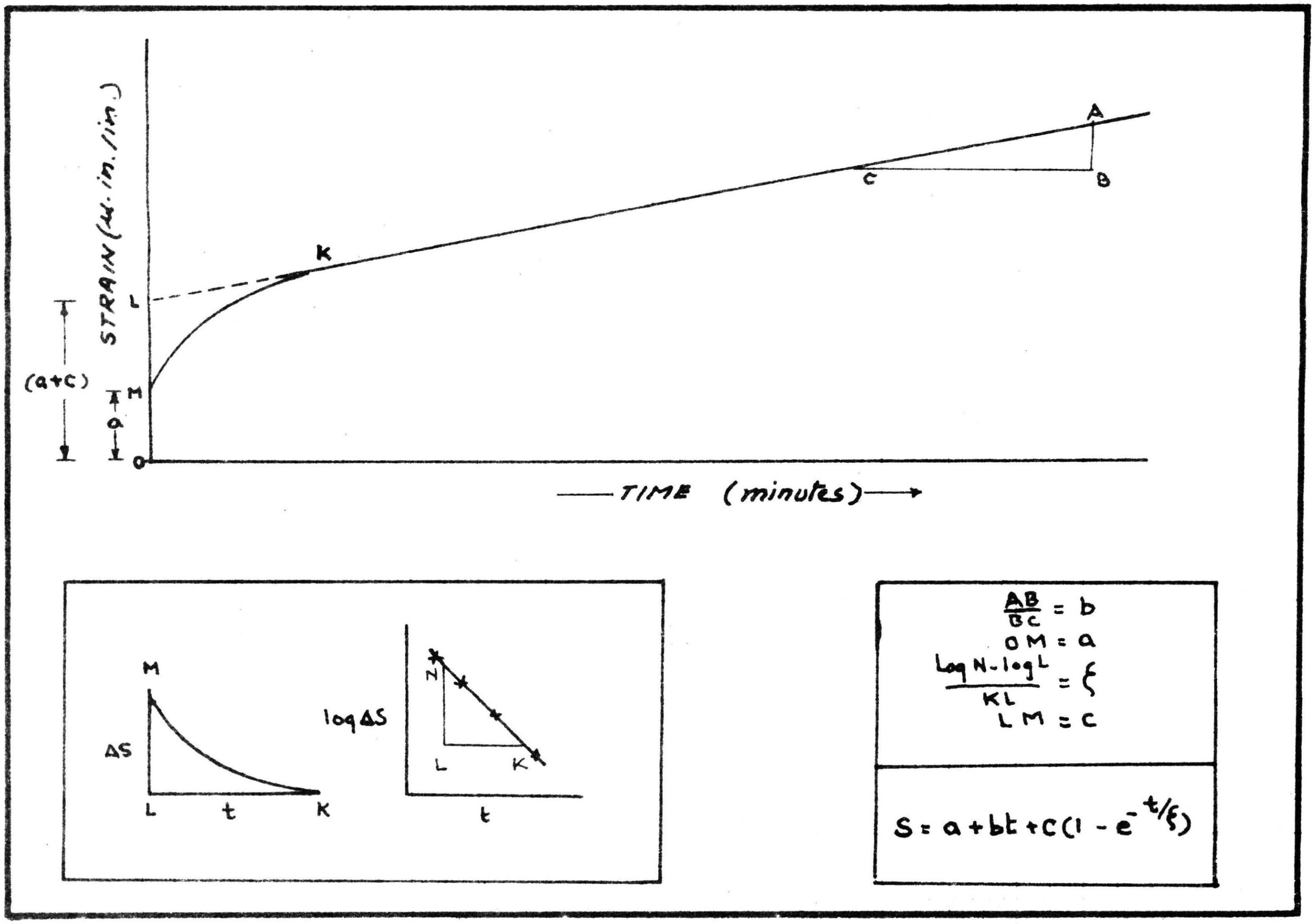

Figure 31. Graphical Determination of Elastico-Viscous Coefficients

Figure 32-a Coefficients A,B,and C for various static loads.

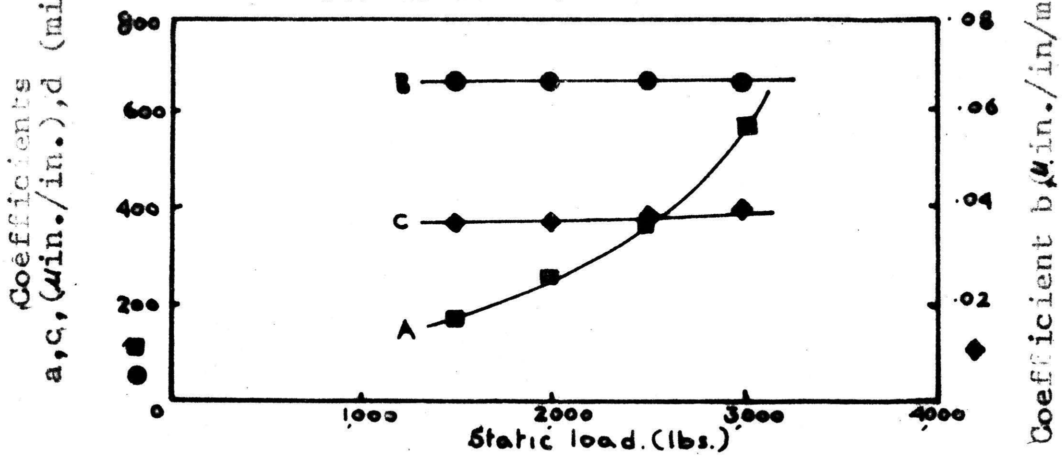

Figure 32-b Viscoelastic coefficients a,b,c and d for various static load levels.

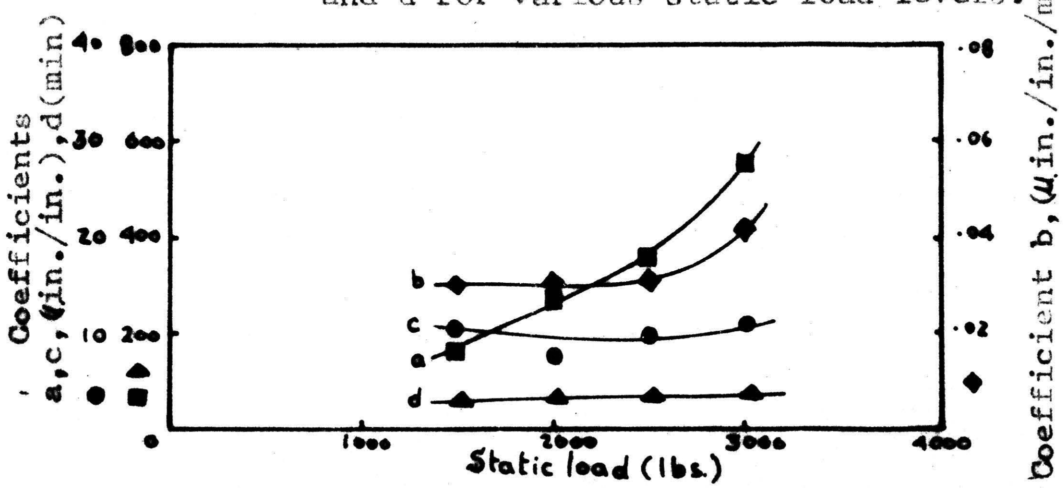

Figure 32-c Effect of static loads on viscoelastic coefficients a,b,c and d at a constant dynamic load.

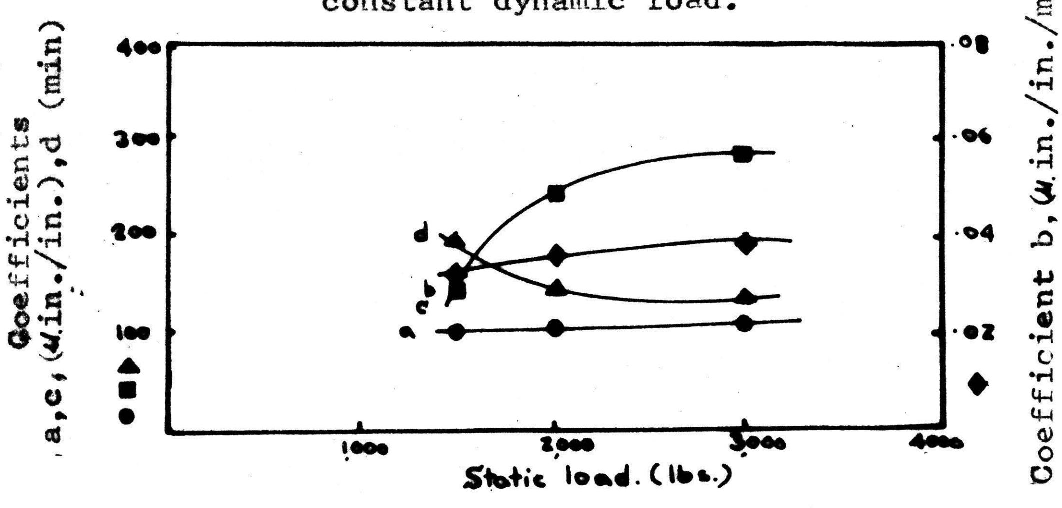

Figure 33-a. Effect of drop heights on viscoelastic coefficients a,b,c and d.

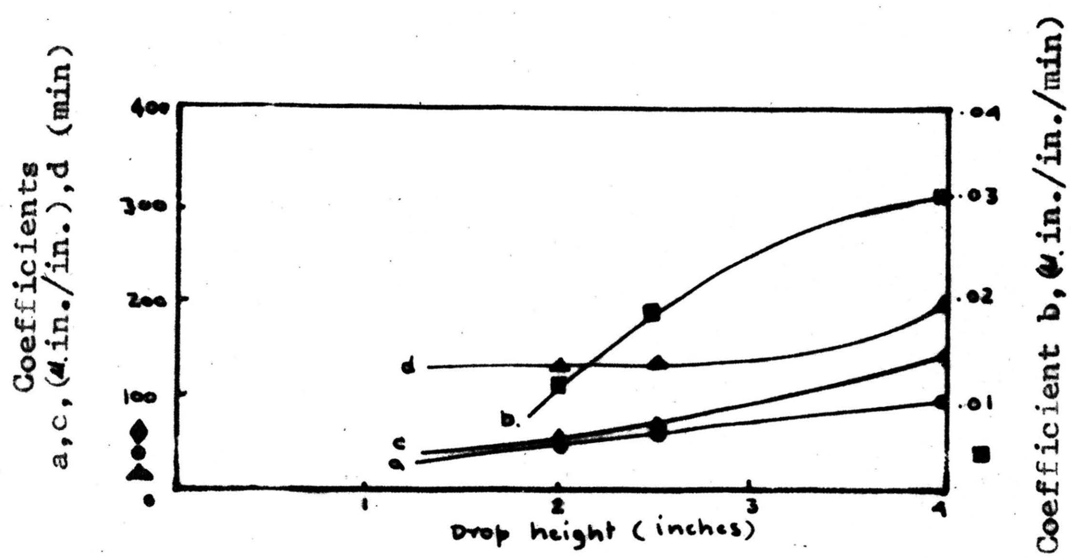

Figure 33-b. Effect of dynamic loads on viscoelastic coefficients a,b,c and d.

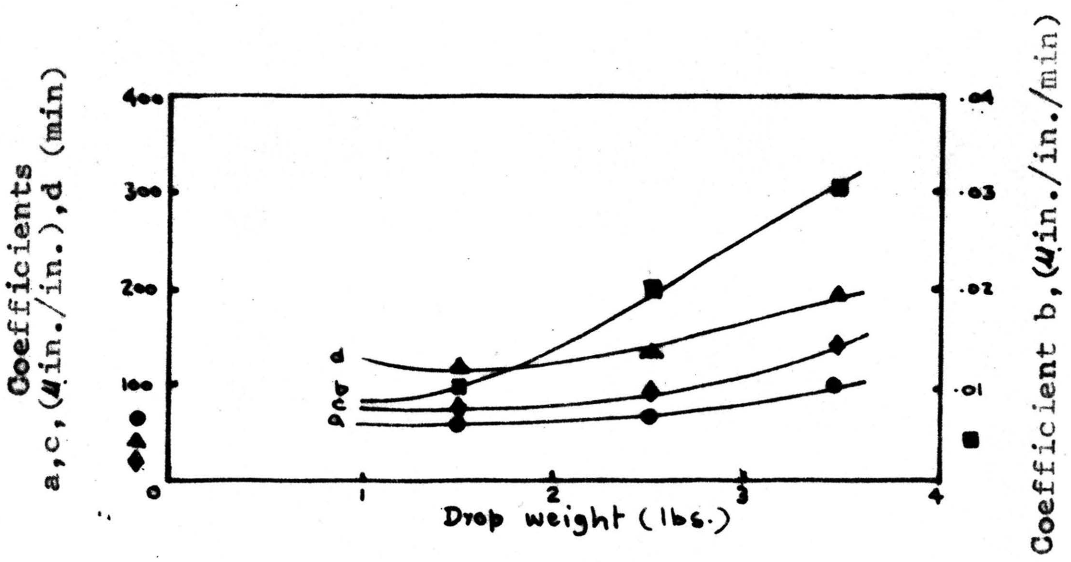

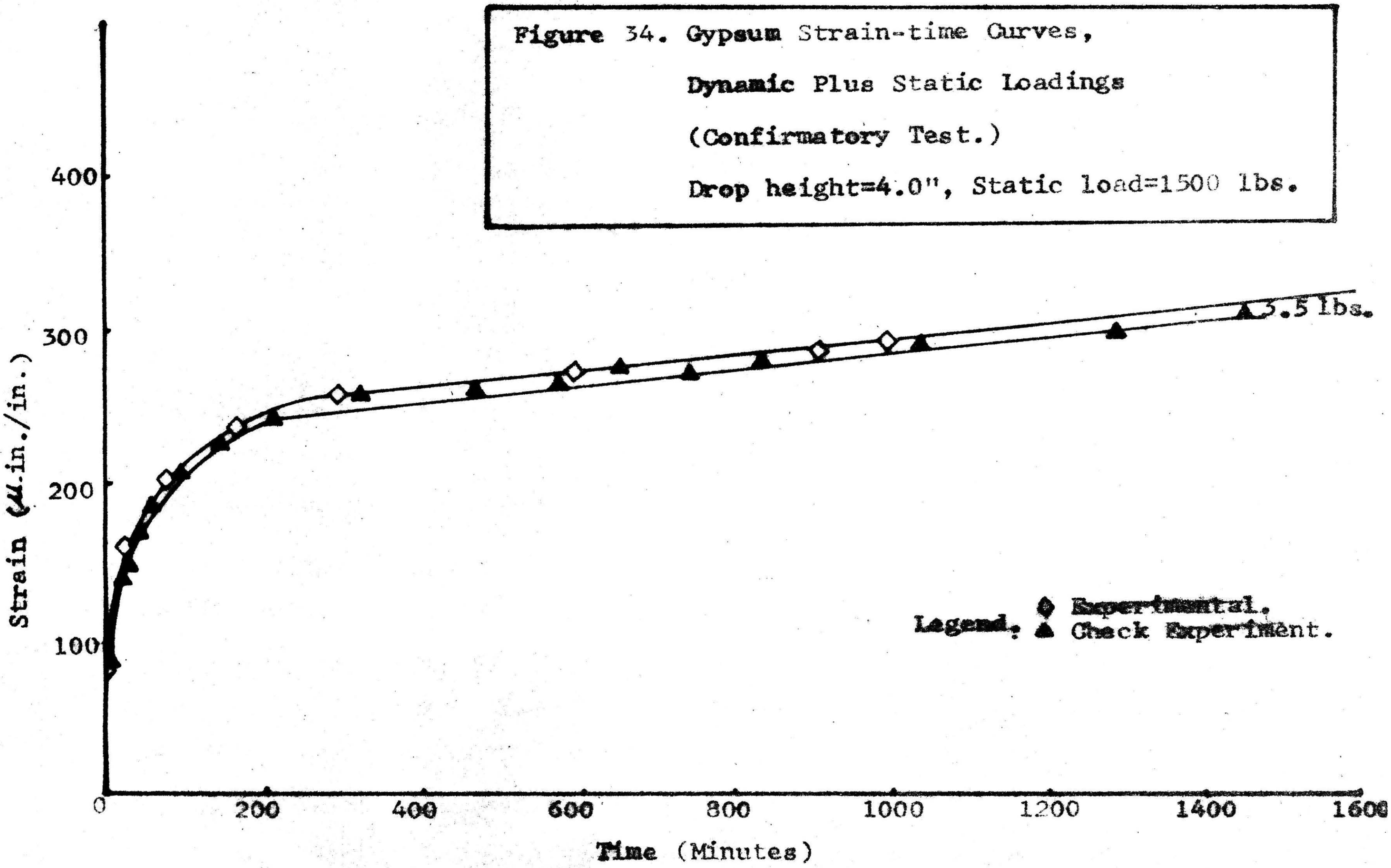

Figure 34. Gypsum Strain-time Curves,
Dynamic Plus Static Loadings
(Confirmatory Test.)
Drop height=4.0", Static load=1500 lbs.

Figure 35. Effect of Momentum on Viscoelastic Coefficients a, b, c, and d, at a Constant Static Load.

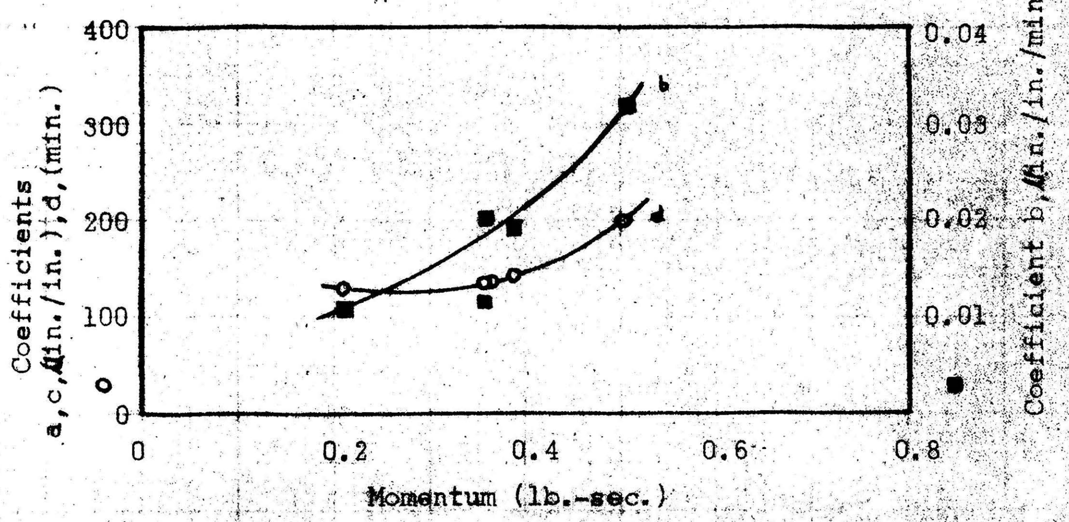

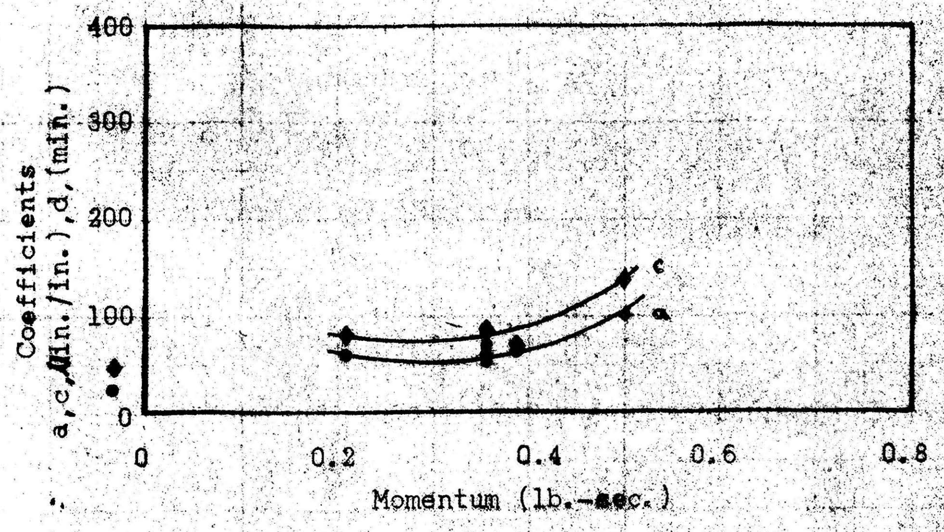

Geologic Description of Gypsum Specimens

The gypsum rock used for experimental purposes was obtained from the Shoals mine of U. S. Gypsum Company. Gypsum in this particular mine occurs as a bedded deposit. It is within the St. Louis limestone of the Meramecians Series; Mississippian System. The average thickness of the gypsum bed is less than 20 feet. The overlying materials are interbedded with limestone and sandstone.

The average thickness of the overburden in this area is roughly 400 feet. The upper part of gypsum is composed of fine grained, hard, and compacted brownish mudstone; a few feet in thickness. Next below the mudstone, there lies a mixture of mudstone and gypsum, containing approximately 50 percent gypsum. In the middle part of the gypsum bed, snow white, clean crystalline gypsum of nearly 90 percent purity occurs. In the lower part mudstone occurs as spots, lenses, and in other irregular shapes, intermingled with gypsum. Small fissures and fractures occur within these gypsum rocks. The contacts between mudstone and gypsum are weak, although no obvious shear zones were apparent. Most of the specimens prepared for this investigation contained medium grained, well crystallized gypsum. A few of the test specimens contained of mudstone lenses in a heterogeneous mixture primarily composed of gypsum.

BIBLIOGRAPHY

1. Andrade, E. N. Dac. (1910), On Viscous Flow in Metals and Allied Phenomens. Proceeding Royal Society, A, Volume 84, p. 1.

2. Burgers, J. M. (1939), Mechanical Considerations - Model Systems - Phenomenological Theories of Relaxation and of Viscosity, First Report on Viscosity and Plasticity, Volume XV, No. 3.

3. Campbell, J. D. (1953), An Investigation of the Plastic Behavior of Metal Rods Subjected to Longitudinal Impact, Journal of Mechanics and Physics of Solids Volume 1, pp. 113-123.

4. Davis, M., and Thompson, N. (1950), Creep in a Precipitation-Hardened Alloy, Proceedings Physics Society B, Volume 63, p. 847.

5. Dushman, S., Dunbar, L. W., and Hutsteiner, H. (1944), Creep of Metals, Journal of Applied Physics, Volume 15, p. 108.

6. Duwez, P. E., and Clark, D. S. (1947), An Experimental Study of the Propagation of Plastic Deformation under Conditions of Longitudinal Impact, A.S.T.M. Proceedings, Volume 47, pp. 502-522.

7. Greenwood, J. N. (1949), The Influence of Vibration on Creep of Lead, A.S.T.M. Proceedings, Volume 49, pp. 834-850.

8. Griggs, D. T. (1936), Deformation of Rocks under High Pressures, Journal of Geology, Volume 44, p. 558.

9. __________ (1939), Creep of Rocks, Journal of Geology, Volume 47, pp. 225-251.

10. __________ (1940), Experimental Flow of Rocks under Conditions Favoring Recrystallization, Geol. Society of America Bull., Volume 51, p. 1012.

11. __________ (1954), Handbook of Physical Constants, Geological Society of America, Special Paper, No. 6, p. 129.

12. Hardy, H. R., (1958), Initial Creep Experiments Using a Hydraulic Loading System, Canadian Department, Mines & Tech., Surveys, Fuel Research Labs, Mines Branch, T.M. 19/58 Min.

13. __________, (1958), Viscoelastic Properties of Geologic Materials, Canadian Department, Mines & Tech., Surveys, Fuel Research Labs, Mines Branch, T.M. 87/58 MIN.

14. __________, (1959), Time Dependent Deformation and Failure of Geologic Materials, Quarterly Colorado School of Mines, Volume 54, No. 3, p. 366.

15. Handin, J. W., and Hager, R. V., Jr. (1957), Experimental Deformation of Sedimentary Rocks under Confining Pressure, American Association of Petroleum Geologists, Bull. 41, p. 1.

16. Jeffreys, H. (1929), The Earth, New York MacMillan Co., Second Edition, p. 265.

17. Landauer, J. K. (1958), The Creep of Snow under Combined Stress, Transactions Society of Rheology, Volume II, pp. 175-194.

18. Lazan, B. T. (1949), Dynamic Creep and Rupture Properties of Temperature Resistant Materials under Tensile Fatique Stress, A.S.T.M. Proceedings, Volume 49, pp. 757-787.

19. Lomnitz, C. (1956), Creep Measurements in Igneous Rocks, Journal of Geology, Volume 64, p. 473.

20. Mann, H. C. (1935), The Relation between the Tension Static and Dynamic Tests, A. S. T. M. Proceedings, Volume 35, pp. 323-335.

21. McAdam, D. J., Jr., and Clyne, R. W. (1938), The Theory of Impact Testing, Influence of Temperature, Velocity of Deformation, Form and Size of Specimen on Work of Deformation, A. S. T. M. Proceedings, Volume 38, pp. 113-132.

22. McVetty, P. G. (1943), Creep of Metals at Elevated Temperatures, Trans. A. S. M. E., Volume 65, pp. 761-769.

23. Phillips, F. (1905), The Slow Stretch in India Rubber, Glass and Metal Wires Subjected to a Constant Pull., Philosophical Magazine, Volume 9, p. 513.

24. Poa, H. Y., and Marin, J. (1954), A New Dynamic Creep Testing Machine, Proc. Expt. Stress Analysis, Volume XI, No. 2, pp. 107-114.

25. Pomeroy, C. D. (1955), The Observation of Creep in Coal at Room Temperature, Br. Nat. Coal Board, Min. Research Establishment, Report 2031.

26. Ross, A. D. (1958), Elasticity, Creep and Shrinkage of Concrete; Mechanical Properties of Non-Metallic Brittle Materials; London, Butterworks Scientific Publication, p. 1.

27. Russell, C. A., (1935), Crystal Growth and Solution under Local Stress, Am. Mineral., Volume 20, pp. 733-737.

28. Saal, R. N. J., and Labout, J. W. A. (1958), Rehology, Theory and Applications, Volume II, Academic Press, Inc., Publishers, New York.

29. Sherby, O. D., and Dorn, J. B. (1958), An Elastic Creep of Polymethyl Methacrylate, Journal, Mech. and Physics Solids, Volume 6, p. 145.

30. Terry, N. B. (1957), The Elastic Properties of Coal, Part 6, Some Measurements of Internal Damping and Some Considerations of Viscoelastic Behavior, Br. Nat. Coal Board, Min. Research Establishment, Report 2080.

31. __________, (1956), The Elastic Properties of Coal, Part 2, Measurement by Means of a Dynamic Resonance Method, Br. Nat. Coal Board, Min. Research Establishment, Report 2048.

32. __________, (1957), Some Considerations of the Magnetostrictive Composite Oscillator Method for Measurement of Elastic Moduli, Br. Jour. of Applied Physics, Volume 8, p. 270.

33. Ward, A. G., and Saunders, P. R. (1958), Rheology, Theory and Applications, Vol. II, Academic Press, Inc., Publishers, New York.

VITA

Ikram-ul-Haq Dar, son of Dr. and Mrs. Abdul Haq was born on January 3, 1936 at Hydrabad Sind, Pakistan.

He received his elementary and secondary education at various government institutes in Pakistan. Upon graduating from Government High School, Sargodha, the author registered at Government College, Lahore, Pakistan. He received an Intermediate Degree in Science in 1952, and studied History and Politics at the same institution for an additional two years.

In 1954, he registered at Government College of Engineering and Technology, Lahore, Pakistan, from which he received a B. S. degree in Mining Engineering in 1957. He was appointed Lecturer, class I at the College of Engineering and Technology the same year and was sent to the United States on a deputation for higher education under the I.C.A. exchange program. The author received a B. S. degree in Geology from Washington State University in 1959.

In September, 1959, he enrolled for graduate study in the Department of Mining Engineering, Missouri School of Mines and Metallurgy, Rolla, Missouri.